

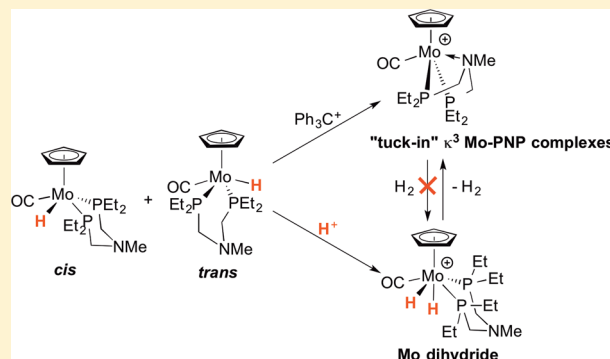
Molybdenum Hydride and Dihydride Complexes Bearing Diphosphine Ligands with a Pendant Amine: Formation of Complexes with Bound Amines

Shaoguang Zhang and R. Morris Bullock*

Physical Sciences Division, Pacific Northwest National Laboratory, P.O. Box 999, K2-12, Richland, Washington 99352, United States

S Supporting Information

ABSTRACT: $\text{CpMo}(\text{CO})(\text{PNP})\text{H}$ complexes ($\text{PNP} = (\text{R}_2\text{PCH}_2)_2\text{NMe}$, $\text{R} = \text{Et}$ or Ph) were synthesized by displacement of two CO ligands of $\text{CpMo}(\text{CO})_3\text{H}$ by the PNP ligand; these complexes were characterized by IR and variable temperature ^1H and ^{31}P NMR spectroscopy. $\text{CpMo}(\text{CO})(\text{PNP})\text{H}$ complexes are formed as mixture of *cis*- and *trans*-isomers. The structures of both *cis*- $\text{CpMo}(\text{CO})(\text{P}^{\text{Et}}\text{N}^{\text{Me}}\text{P}^{\text{Et}})\text{H}$ and *trans*- $\text{CpMo}(\text{CO})(\text{P}^{\text{Ph}}\text{N}^{\text{Me}}\text{P}^{\text{Ph}})\text{H}$ were determined by single crystal X-ray diffraction. Electrochemical oxidation of $\text{CpMo}(\text{CO})(\text{P}^{\text{Et}}\text{N}^{\text{Me}}\text{P}^{\text{Et}})\text{H}$ and $\text{CpMo}(\text{CO})(\text{P}^{\text{Ph}}\text{N}^{\text{Me}}\text{P}^{\text{Ph}})\text{H}$ in CH_3CN are both irreversible at slow scan rates and quasireversible at higher scan rates, with $E_{1/2} = -0.36$ V (vs $\text{Cp}_2\text{Fe}^{+/0}$) for $\text{CpMo}(\text{CO})(\text{P}^{\text{Et}}\text{N}^{\text{Me}}\text{P}^{\text{Et}})\text{H}$ and $E_{1/2} = -0.18$ V for $\text{CpMo}(\text{CO})(\text{P}^{\text{Ph}}\text{N}^{\text{Me}}\text{P}^{\text{Ph}})\text{H}$. Hydride abstraction from $\text{CpMo}(\text{CO})(\text{PNP})\text{H}$ with $[\text{Ph}_3\text{C}]^+[\text{A}]^-$ ($\text{A} = \text{B}(\text{C}_6\text{F}_5)_4$ or BAr^{F}_4 ; $[\text{Ar}^{\text{F}} = 3,5\text{-bis}(\text{trifluoromethyl})\text{phenyl}]$) afforded “tuck-in” $[\text{CpMo}(\text{CO})(\kappa^3\text{-PNP})]^+$ complexes that feature the amine bound to the metal. Displacement of the κ^3 Mo–N bond by CD_3CN gives $[\text{CpMo}(\text{CO})(\text{PNP})(\text{CD}_3\text{CN})]^+$. The kinetics of this reaction were studied by $^{31}\text{P}\{^1\text{H}\}$ NMR spectroscopy for $[\text{CpMo}(\text{CO})(\kappa^3\text{-P}^{\text{Et}}\text{N}^{\text{Me}}\text{P}^{\text{Et}})]^+$, providing the activation parameters $\Delta H^\ddagger = 21.6 \pm 2.8$ kcal/mol, $\Delta S^\ddagger = -0.3 \pm 9.8$ cal/(mol K), $E_a = 22.1 \pm 2.8$ kcal/mol. Protonation of $\text{CpMo}(\text{CO})(\text{P}^{\text{Et}}\text{N}^{\text{Me}}\text{P}^{\text{Et}})\text{H}$ affords the Mo dihydride complex $[\text{CpMo}(\text{CO})(\kappa^2\text{-P}^{\text{Et}}\text{N}^{\text{Me}}\text{P}^{\text{Et}})(\text{H})_2]^+$, which loses H_2 to generate $[\text{CpMo}(\text{CO})(\kappa^3\text{-P}^{\text{Et}}\text{N}^{\text{Me}}\text{P}^{\text{Et}})]^+$ at room temperature. Our results show that the pendant amine has a strong driving force to form stable “tuck-in” $[\text{CpMo}(\text{CO})(\kappa^3\text{-PNP})]^+$ complexes, and also promotes hydrogen elimination from $[\text{CpMo}(\text{CO})(\text{PNP})(\text{H})_2]^+$ complexes by formation of a Mo–N dative bond. $\text{CpMo}(\text{CO})(\text{dppp})\text{H}$ ($\text{dppp} = 1,3\text{-bis}(\text{diphenylphosphino})\text{propane}$) was studied as a Mo diphosphine analogue without a pendant amine, and the product of protonation of this complex gives $[\text{CpMo}(\text{CO})(\text{dppp})(\text{H})_2]^+$.

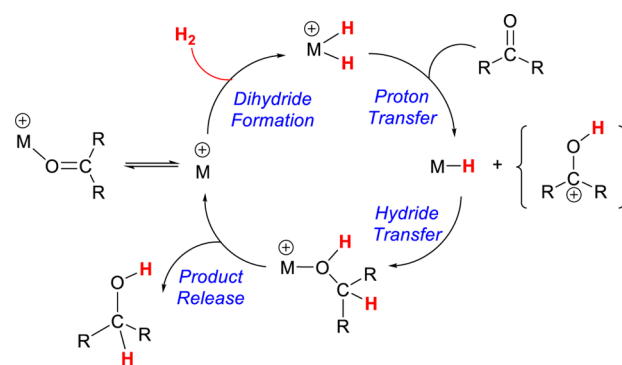


■ INTRODUCTION

Metal hydride complexes are important in many catalytic transformations, such as ionic hydrogenation, hydrogen oxidation, and hydrogen production.¹ In the process of delivering hydrogen to organic substrates from a metal hydride complex, both proton transfer and hydride transfer reactions are fundamental and crucial.² We have extensively studied half-sandwich cyclopentadienyl molybdenum and tungsten complexes bearing phosphine or *N*-heterocyclic carbene ligands for catalytic ionic hydrogenations or hydrosilylation of ketones.^{1a,b,3} In these reactions, proton transfer from a cationic dihydride to the ketone is followed by hydride transfer from a neutral metal hydride,⁴ creating a vacant coordination site on the metal that can react with other ligands. Reaction with H_2 generates the metal dihydride complexes (Scheme 1). Thus, tuning both the acidity and hydricity of metal hydride and dihydride complexes influences the kinetics and thermodynamics of proton and hydride transfers as well as the overall catalytic activity.

We previously reported the synthesis and reactions of $\text{CpMo}(\text{CO})(\text{dppe})\text{H}$ ($\text{dppe} = \text{Ph}_2\text{PCH}_2\text{CH}_2\text{PPh}_2$).⁵ Incorporating

Scheme 1



rating a pendant amine into the diphosphine ligand leads to the possibility of the pendant amine functioning as a proton relay, to accelerate intramolecular and/or intermolecular proton

Received: March 31, 2015

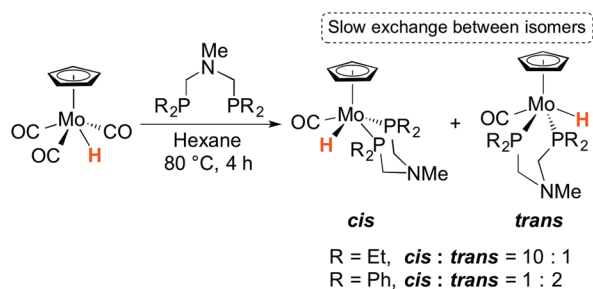
Published: June 8, 2015

transfer reactions.⁶ In contrast to the previously studied metal dihydride complexes, the pendant amine allows the separation of site of the proton donor from the hydride donor, and thus, it may be possible to tune their electronic effects separately. The study of the active site of [FeFe]-hydrogenase and synthetic metal complexes that mimic hydrogenase reactivity has shown that pendant amines promote intramolecular proton relay and heterolytic cleavage of hydrogen.^{6d,k,7} Herein we report the synthesis, structures, and electrochemical oxidation of CpMo(CO)(PNP)H (PNP = (R₂PCH₂)₂NMe), complexes bearing a diphosphine ligand with a pendant amine. We found that hydride abstraction from CpMo(CO)(PNP)H gives a “tuck-in” [CpMo(CO)(κ³-PNP)]⁺ complex that features a bound pendant amine. Protonation of CpMo(CO)(PNP)H gives the dihydride complex [CpMo(CO)(PNP)(H)₂]⁺, which has been characterized by an X-ray crystal structure and NMR spectroscopy. We show that the pendant amine is the key factor in formation of “tuck-in” [CpMo(CO)(κ³-PNP)]⁺ complexes and hydrogen elimination from [CpMo(CO)(PNP)(H)₂]⁺ complexes. An analogous CpMo(CO)(dppp)H (dppp = 1,3-bis(diphenylphosphino)propane) complex and its corresponding dihydride complex are also described.

RESULTS AND DISCUSSION

Synthesis and Structure of CpMo(CO)(PNP)H. We developed convenient synthetic procedures for the synthesis of molybdenum hydride complexes CpMo(CO)(PNP)H (Scheme 2, PNP = (R₂PCH₂)₂NMe). The reaction of

Scheme 2



Et₂PCH₂NMeCH₂PEt₂ (P^{Et}N^{Me}P^{Et})^{6d} with CpMo(CO)₃H in hexane at 80 °C readily afforded light yellow crystalline CpMo(CO)(P^{Et}N^{Me}P^{Et})H in 70% isolated yield. When the diphosphine Ph₂PCH₂NMeCH₂PPh₂ (P^{Ph}N^{Me}P^{Ph})⁸ was used instead of P^{Et}N^{Me}P^{Et}, CpMo(CO)(P^{Ph}N^{Me}P^{Ph})H precipitated from the hexane solution as a yellow powder that was isolated in 63% yield.

Ligand substitution of CO of CpMo(CO)₃H by PR₃ provides an excellent synthetic method for CpMo(CO)₂(PR₃)H (R = Me, Cy, Ph).^{4a,9} Our straightforward synthesis of CpMo(CO)(PNP)H directly from CpMo(CO)₃H and PNP offers advantages over the synthesis previously reported⁵ for cis-CpMo(CO)(dppe)H by reduction of cis-CpMo(CO)(dppe)Cl with Na⁺[AlH₂(OCH₂CH₂OCH₃)₂][−]. The reaction of CpMo(CO)₃H with dppe gave CpMo(CO)₂(κ¹-dppe)H as the predominant product instead of the desired product, CpMo(CO)(κ²-dppe)H,⁵ that results from displacement of two CO ligands. PNP ligands have more flexibility, forming a six-membered Mo-PNP ring instead of five-membered ring for CpMo(CO)(dppe)H. Thus, the larger

bite angle of the Mo-PNP ring likely contributes to the successful synthesis of CpMo(CO)(PNP)H.

Spectroscopic Characterization of CpMo(CO)(PNP)H. Both CpMo(CO)(P^{Et}N^{Me}P^{Et})H and CpMo(CO)(P^{Ph}N^{Me}P^{Ph})H were characterized by ¹H, ³¹P, and ¹³C NMR spectroscopy. The hydride of CpMo(CO)(P^{Et}N^{Me}P^{Et})H displays two resonances at 20 °C in the ¹H NMR spectrum in toluene-*d*₈ (Figure 1). A triplet at −8.00 ppm (²J_{HP} = 71 Hz) was assigned

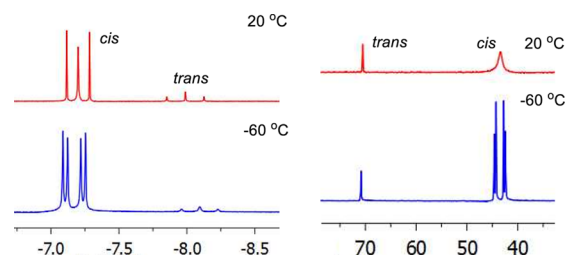


Figure 1. ¹H NMR spectra of the Mo–H resonance (left) and ³¹P{¹H} NMR spectra (right) of *cis*- and *trans*-CpMo(CO)-(P^{Et}N^{Me}P^{Et})H at 20 °C and −60 °C in toluene-*d*₈.

to the *trans*-isomer, as this isomer exhibits a coupling constant consistent with coupling of the hydride *cis* to two phosphines. Note that, in the nomenclature used here, *cis* or *trans* refers to the geometry of the H and CO ligands; they are not strictly *cis* or *trans* as in an octahedral complex, but this description follows that normally used for complexes with four-legged piano-stool geometries. The hydride of the *cis*-isomer showed a pseudotriplet at −7.20 ppm (²J_{HP} = 41 Hz), with a much smaller ²J_{HP} than that of the *trans*-isomer. We attribute the triplet resonance and smaller ²J_{HP} for the *cis*-isomer to the fluxional behavior of carbonyl and hydride ligands at higher temperature. The exchange of carbonyl and hydride in the *cis*-isomer is faster than the NMR time scale, which causes averaging of the coupling constant of hydride to the *cis*- and *trans*-phosphine.¹⁰ At −60 °C, the hydride resonance for *trans*-CpMo(CO)(P^{Et}N^{Me}P^{Et})H still shows a triplet with the same ²J_{HP} coupling constant in ¹H NMR spectrum, but the hydride of the *cis*-isomer transforms from a pseudotriplet to a doublet of doublets, providing ²J_{HP} ≈ 19 Hz for the coupling of the hydride to the *trans*-phosphine and ²J_{HP} ≈ 68 Hz for the coupling of the hydride to the *cis*-phosphine. The magnitude of these coupling constants is comparable to those observed in interconverting *cis/trans* isomer mixtures of related monophosphine hydride complexes CpMo(CO)₂(PPh₃)H (²J_{HP} = 21 Hz for *trans*; ²J_{HP} = 64 Hz for *cis*)^{10,11} and diphosphine hydride complexes CpMo(CO)(dppe)H (²J_{HP} = 16 Hz for *trans*; ²J_{HP} = 69 Hz for *cis*).⁵ This result indicates the fluxional behavior of the *cis*-isomer slows down at low temperature. On the basis of integration of metal hydride resonances, the ratio of *cis:trans* isomers of CpMo(CO)(P^{Et}N^{Me}P^{Et})H was 10:1. The ³¹P{¹H} NMR spectrum of CpMo(CO)(P^{Et}N^{Me}P^{Et})H at 20 °C in toluene also shows two phosphorus resonances. The singlet at 70.5 ppm is assigned to the phosphorus atoms in the symmetrical structure of the *trans*-isomer. The ³¹P{¹H} NMR spectrum of the *cis*-isomer appears as a broad singlet at 43.4 ppm due to its fluxional behavior. This broad singlet is transformed into two doublets at 44.4 and 42.4 ppm (²J_{PP} = 71 Hz) at −60 °C.

Similarly, the hydride of CpMo(CO)(P^{Ph}N^{Me}P^{Ph})H also displays two resonances at 20 °C in the ¹H NMR spectrum in toluene-*d*₈. The triplet at −6.69 ppm (²J_{HP} = 70 Hz) is assigned

Table 1. IR Data ($\tilde{\nu}_{\text{CO}}$, cm^{-1}) in Solution

complex	hexane	PhF	MeCN	CH_2Cl_2
$\text{CpMo}(\text{CO})(\text{P}^{\text{Et}}\text{N}^{\text{Me}}\text{P}^{\text{Et}})\text{H}$	1844 (<i>cis</i>) 1813 (<i>trans</i>)	1819		
$\text{CpMo}(\text{CO})(\text{P}^{\text{Ph}}\text{N}^{\text{Me}}\text{P}^{\text{Ph}})\text{H}$		1810		1804
$[\text{CpMo}(\text{CO})(\kappa^3\text{-P}^{\text{Et}}\text{N}^{\text{Me}}\text{P}^{\text{Et}})]^+[\text{B}(\text{C}_6\text{F}_5)_4]^-$		1844		
$[\text{CpMo}(\text{CO})(\kappa^2\text{-P}^{\text{Et}}\text{N}^{\text{Me}}\text{P}^{\text{Et}})(\text{N}\equiv\text{CCD}_3)]^+[\text{BAr}^{\text{F}}_4]^-$			1855	
$[\text{CpMo}(\text{CO})(\kappa^3\text{-P}^{\text{Ph}}\text{N}^{\text{Me}}\text{P}^{\text{Ph}})]^+[\text{B}(\text{C}_6\text{F}_5)_4]^-$		1859		
$[\text{CpMo}(\text{CO})(\kappa^2\text{-P}^{\text{Et}}\text{N}^{\text{Me}}\text{P}^{\text{Et}})(\text{H})_2]^+[\text{B}(\text{C}_6\text{F}_5)_4]^-$		2037		
$\text{CpMo}(\text{CO})(\kappa^2\text{-dppp})\text{H}$		1813		
$[\text{CpMo}(\text{CO})(\kappa^2\text{-dppp})(\text{H})_2]^+[\text{B}(\text{C}_6\text{F}_5)_4]^-$		1982		

to the hydride of the *trans*-isomer, and the coupling constant is independent of temperature. The pseudotriplet at -5.65 ppm with a smaller $^2J_{\text{HP}} = 41$ Hz is assigned to hydride of the *cis*-isomer, which transformed at -60 °C to a doublet of doublets, providing values of $^2J_{\text{HP}} \cong 48$ and 34 Hz for the coupling of the hydride to the *cis*- and *trans*-phosphine, respectively. On the basis of integration of metal hydride resonances in the ^1H NMR spectrum, the ratio of the *cis*:*trans* isomer was 1:2. Thus, the *trans*-isomer is favored for $\text{CpMo}(\text{CO})(\text{P}^{\text{Ph}}\text{N}^{\text{Me}}\text{P}^{\text{Ph}})\text{H}$, whereas the *cis*-isomer predominated for $\text{CpMo}(\text{CO})(\text{P}^{\text{Et}}\text{N}^{\text{Me}}\text{P}^{\text{Et}})\text{H}$. The $^{31}\text{P}\{^1\text{H}\}$ NMR spectrum of *trans*- $\text{CpMo}(\text{CO})(\text{P}^{\text{Ph}}\text{N}^{\text{Me}}\text{P}^{\text{Ph}})\text{H}$ shows a singlet at 74.1 ppm at 20 °C in toluene- d_8 , suggesting a symmetrical structure. The phosphorus resonance of *cis*- $\text{CpMo}(\text{CO})(\text{P}^{\text{Ph}}\text{N}^{\text{Me}}\text{P}^{\text{Ph}})\text{H}$ shows a singlet at 51.1 ppm in the $^{31}\text{P}\{^1\text{H}\}$ NMR spectrum at 20 °C, which is transformed into two doublets at -60 °C ($^2J_{\text{PP}} = 52, 61$ Hz), again suggesting the fluxional behavior of the *cis*-isomer slows down at low temperature. See the Supporting Information for ^1H and ^{31}P NMR spectra of the Mo–H resonance of $\text{CpMo}(\text{CO})(\text{P}^{\text{Ph}}\text{N}^{\text{Me}}\text{P}^{\text{Ph}})\text{H}$ at 20 °C and -60 °C.

The ratio of *cis*- and *trans*-isomers is independent of temperature. Heating $\text{CpMo}(\text{CO})(\text{P}^{\text{Et}}\text{N}^{\text{Me}}\text{P}^{\text{Et}})\text{H}$ or $\text{CpMo}(\text{CO})(\text{P}^{\text{Ph}}\text{N}^{\text{Me}}\text{P}^{\text{Ph}})\text{H}$ in C_6D_6 for 16 h at 80 °C led to no change in the ^1H NMR spectrum or the ratio of integration of metal hydride resonances of the *cis*- and *trans*-isomers. These results also indicate that both $\text{CpMo}(\text{CO})(\text{PNP})\text{H}$ complexes are thermally stable.

The IR spectrum of $\text{CpMo}(\text{CO})(\text{P}^{\text{Et}}\text{N}^{\text{Me}}\text{P}^{\text{Et}})\text{H}$ in hexane shows carbonyl stretching bands ($\tilde{\nu}_{\text{CO}}$) at 1844 and 1813 cm^{-1} , which are assigned to the *cis*- and *trans*-isomers, respectively (Table 1). The relative intensities are consistent with this assignment. In fluorobenzene, only one $\tilde{\nu}_{\text{CO}}$ is observed, at 1819 cm^{-1} . $\text{CpMo}(\text{CO})(\text{P}^{\text{Ph}}\text{N}^{\text{Me}}\text{P}^{\text{Ph}})\text{H}$ is sparingly soluble in hexane, but dissolves readily in aromatic and in polar solvents. The IR spectra in fluorobenzene and CH_2Cl_2 (Table 1) both show one carbonyl stretching band ($\tilde{\nu}_{\text{CO}}$) at 1810 and 1804 cm^{-1} , respectively. A $\tilde{\nu}(\text{M}–\text{H})$ stretching band of $\text{CpMo}(\text{CO})(\text{P}^{\text{Et}}\text{N}^{\text{Me}}\text{P}^{\text{Et}})\text{H}$ was found in hexane solution as a weak band at 1942 cm^{-1} .

Crystallographic Characterization of $\text{CpMo}(\text{CO})(\text{PNP})\text{H}$. Light yellow single crystals of *cis*- $\text{CpMo}(\text{CO})(\text{P}^{\text{Et}}\text{N}^{\text{Me}}\text{P}^{\text{Et}})\text{H}$ were grown by evaporating a hexane solution at room temperature overnight. Yellow single crystals of *trans*- $\text{CpMo}(\text{CO})(\text{P}^{\text{Ph}}\text{N}^{\text{Me}}\text{P}^{\text{Ph}})\text{H}$ were grown by evaporating a solution of fluorobenzene and hexane (1:1) at room temperature. Both *cis*- $\text{CpMo}(\text{CO})(\text{P}^{\text{Et}}\text{N}^{\text{Me}}\text{P}^{\text{Et}})\text{H}$ and *trans*- $\text{CpMo}(\text{CO})(\text{P}^{\text{Ph}}\text{N}^{\text{Me}}\text{P}^{\text{Ph}})\text{H}$ were analyzed by single crystal X-ray diffraction (Figure 2). Selected bond distances and angles are provided in Table 2. The crystal structure of *cis*- $\text{CpMo}(\text{CO})(\text{P}^{\text{Et}}\text{N}^{\text{Me}}\text{P}^{\text{Et}})\text{H}$ shows a four-legged piano-stool geometry. The six-membered Mo–PNP ring adopts a chair conformation. The P–Mo–P bond angle of

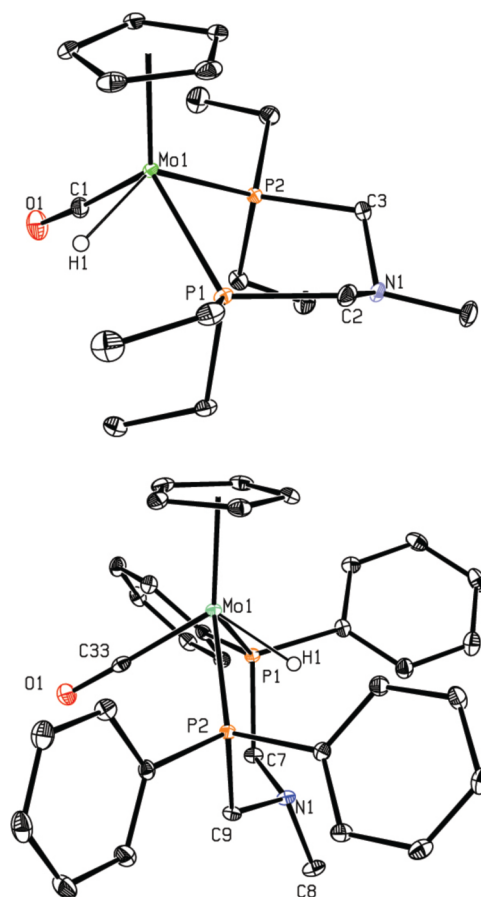


Figure 2. ORTEP drawing of *cis*- $\text{CpMo}(\text{CO})(\text{P}^{\text{Et}}\text{N}^{\text{Me}}\text{P}^{\text{Et}})\text{H}$ (upper) and *trans*- $\text{CpMo}(\text{CO})(\text{P}^{\text{Ph}}\text{N}^{\text{Me}}\text{P}^{\text{Ph}})\text{H}$ (lower) with 30% thermal ellipsoids and hydrogen atoms omitted for clarity, except Mo–H.

$80.283(10)^\circ$ in *cis*- $\text{CpMo}(\text{CO})(\text{P}^{\text{Et}}\text{N}^{\text{Me}}\text{P}^{\text{Et}})\text{H}$ is similar to the P–Mo–P angle of $81.21(4)^\circ$ in $\text{Cp}^*\text{Mo}(\text{dppe})\text{H}_3$,¹³ and slightly larger than the angles of $78.4(1)^\circ$ in *cis*- $\text{CpMo}(\text{CO})(\text{dppe})\text{H}$ and $75.3(1)^\circ$ in *cis*- $\text{CpMo}(\text{CO})(\text{dppe})\text{Cl}$.^{5,14}

The crystal structure of *trans*- $\text{CpMo}(\text{CO})(\text{P}^{\text{Ph}}\text{N}^{\text{Me}}\text{P}^{\text{Ph}})\text{H}$ also shows four-legged piano-stool coordination geometry and an unusual *trans*-geometry of the two phosphines. The P–Mo–P bond angle in *trans*- $\text{CpMo}(\text{CO})(\text{P}^{\text{Ph}}\text{N}^{\text{Me}}\text{P}^{\text{Ph}})\text{H}$ is $97.540(17)^\circ$, which is larger than the P–Mo–P bond angle of $90.70(4)^\circ$ in *trans*- $\text{Cp}^*\text{Mo}(\text{depp})\text{Cl}_2$ (depp = $\text{Et}_2\text{PCH}_2\text{CH}_2\text{CH}_2\text{PEt}_2$),¹⁵ $80.283(10)^\circ$ in *cis*- $\text{CpMo}(\text{CO})(\text{P}^{\text{Et}}\text{N}^{\text{Me}}\text{P}^{\text{Et}})\text{H}$ and $80.60(3)^\circ$ in *trans*- $\text{Cp}^*\text{Mo}(\text{dppe})\text{Cl}_2$,¹² probably due to less ring strain in the larger six-membered Mo–PNP ring than the five-membered Mo–dppe ring. To the best of our knowledge, *trans*-Mo diphosphine complexes are rare.^{12,14,15} Poli and co-workers¹² reported a 17-electron *trans*- $\text{Cp}^*\text{Mo}(\text{dppe})\text{Cl}_2$ complex.

Table 2. Selected Bond Lengths (Å) and Angles (deg) for *cis*-CpMo(CO)(P^{Et}N^{Me}P^{Et})H and *trans*-CpMo(CO)(P^{Ph}N^{Me}P^{Ph})H Complexes^a

	<i>cis</i> -CpMo(CO)(P ^{Et} N ^{Me} P ^{Et})H	<i>trans</i> -CpMo(CO)(P ^{Ph} N ^{Me} P ^{Ph})H
Mo–P (<i>cis</i> to H)	2.4107(3)	2.3505(5), 2.3680(5)
Mo–P (<i>trans</i> to H)	2.3981(3)	
Mo–C(CO)	1.9268(12)	1.9377(18)
C–O	1.1768(14)	1.165(2)
P–Mo–P	80.283(10)	97.540(17)

^aHydride was located on the electron density map.

Hydrides in both two structures were located on the electron density map, but the precise location of hydrides in all of these structures is subject to the uncertainties associated with X-ray crystallography.¹⁶

Electrochemical Characterization of CpMo(CO)(PNP)-H. Electrochemical oxidation of CpMo(CO)(P^{Et}N^{Me}P^{Et})H and CpMo(CO)(P^{Ph}N^{Me}P^{Ph})H was studied by cyclic voltammetry in CH₃CN. At slow scan rates, the oxidation waves of the two complexes are irreversible (Figure 3). The peak potential for

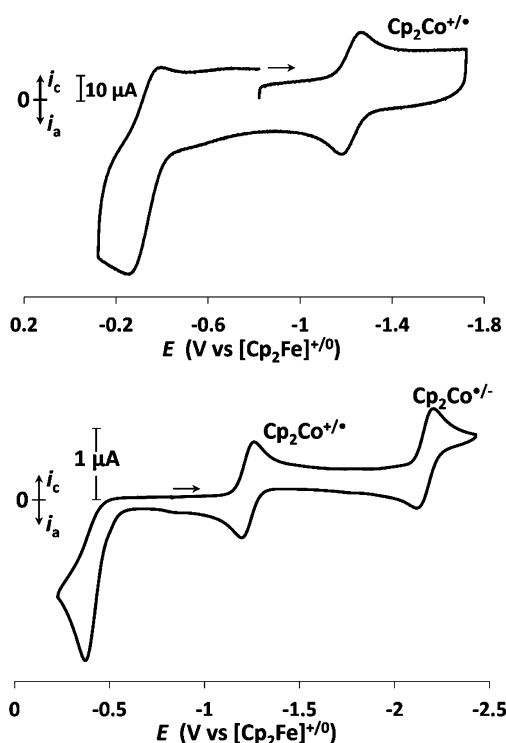


Figure 3. Cyclic voltammograms of CpMo(CO)(P^{Et}N^{Me}P^{Et})H. Conditions: 1 mM CpMo(CO)(P^{Et}N^{Me}P^{Et})H in CH₃CN with 0.2 M [Bu₄N]⁺[PF₆][−]. Upper: $\nu = 36 \text{ V s}^{-1}$. Lower: $\nu = 0.05 \text{ V s}^{-1}$.

the oxidation waves was found at -0.37 V for CpMo(CO)(P^{Et}N^{Me}P^{Et})H and -0.24 V for CpMo(CO)(P^{Ph}N^{Me}P^{Ph})H (vs Cp₂Fe^{+/0}, at $\nu = 0.05 \text{ V s}^{-1}$). At the higher scan rate of 36 V s^{-1} , the oxidation wave of CpMo(CO)(P^{Et}N^{Me}P^{Et})H becomes quasireversible, with a 114 mV peak-to-peak separation (cf., 90 mV for Cp₂Co^{+/•} added as a reference), and gives $E_{1/2} = -0.36 \text{ V}$ (vs Cp₂Fe^{+/0}). This wave is assigned to the [CpMo(CO)(P^{Et}N^{Me}P^{Et})H]^{•+}/CpMo(CO)(P^{Et}N^{Me}P^{Et})H couple. CpMo(CO)(P^{Et}N^{Me}P^{Et})H shows a more negative oxidation potential than CpMo(CO)(dppe)H ($E_p = -0.15 \text{ V}$), as expected, since P^{Et}N^{Me}P^{Et}, with ethyl groups on the phosphine, is a stronger electron donor ligand than dppe. The

oxidation wave of CpMo(CO)(P^{Ph}N^{Me}P^{Ph})H also becomes quasireversible at a scan rate of 49 V s^{-1} , with a 139 mV peak-to-peak separation (cf. 141 mV for Cp₂Co^{+/•}), and gives $E_{1/2} = -0.18 \text{ V}$ (vs Cp₂Fe^{+/0}) (see Supporting Information). This wave is assigned to the [CpMo(CO)(P^{Ph}N^{Me}P^{Ph})H]^{•+}/CpMo(CO)(P^{Ph}N^{Me}P^{Ph})H couple. The oxidation potentials for selected CpMo phosphine hydride complexes are summarized in Table 3.

Table 3. Oxidation Potentials for Selected Mo Phosphine Hydride Complexes in MeCN

	$E_{p,a}/\text{V}^a$ vs Cp ₂ Fe ^{+/0}
CpMo(CO) ₃ H	+0.80 ¹⁷
CpMo(CO) ₂ (PPh ₃)H	+0.26; ¹⁸ +0.23 ¹⁹
CpMo(CO)(dppe)H	−0.15 ⁵
CpMo(CO)(P ^{Ph} N ^{Me} P ^{Ph})H ^b	−0.18 (this work)
CpMo(CO)(P ^{Et} N ^{Me} P ^{Et})H ^b	−0.36 (this work)
CpMo(PMe ₃) ₃ H ^c	−1.46 ²⁰

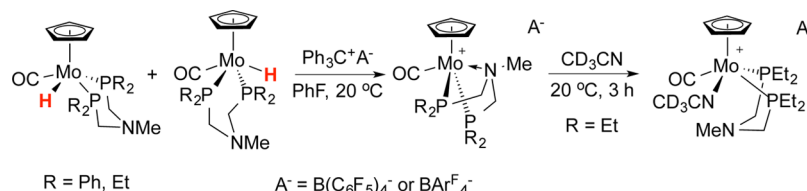
^aPeak potential for oxidation. ^bQuasireversible oxidation. ^c $E_{1/2}$, reversible oxidation.

Formation of Tuck-In [CpMo(CO)(κ³-PNP)]⁺ Complexes by Hydride Abstraction from CpMo(CO)(PNP)H.

We previously reported that hydride abstraction from CpMo(CO)₂(PPh₃)H by [Ph₃C]⁺[A][−] (A[−] = B(C₆F₅)₄[−] or BAR^F₄[−]; Ar^F = 3,5-bis(trifluoromethyl)phenyl) gives [CpMo(CO)₂(κ³-PPh₃)]⁺[B(C₆F₅)₄][−] where the Mo bonds to one C=C bond of a Ph ring of the PPh₃ ligand, as well as the conventional bonding through the phosphine.²¹ Subsequently, we found that hydride abstraction from CpMo(CO)₂(P^{Pr}Pr₃)H afforded agostic C–H bond complexes β- and γ-[CpMo(CO)₂(P^{Pr}Pr₃)]⁺[B(C₆F₅)₄][−],²² where either the methine or the methyl C–H of the isopropyl group forms an agostic bond to the Mo. Both of these results highlight the propensity of the cationic 16-electron Mo fragments to form bonds to any available donor, even weak ones.

We found that treatment of CpMo(CO)(P^RN^{Me}P^R)H (R = Et, Ph) with [Ph₃C]⁺[A][−] (A = B(C₆F₅)₄ or BAR^F₄) in fluorobenzene cleanly afforded [CpMo(CO)(κ³-P^RN^{Me}P^R)]⁺ as “tuck-in” complexes with the amine bound to the metal (Scheme 3). Ligands with pendant amines are generally intended to have the amine function as a proton relay, with the amine *not* bonded to the metal, so metal diphosphine complexes with κ³ bonding of the amine are rare, but have been observed. Previously reported examples include (κ³-P^{Ph}N^{Bn})₂-CrCl₃ (P^{Ph}N^{Bn} = 1,5-diphenyl-3,7-dibenzyl-1,5-diaza-3,7-diphosphacyclooctane),²³ [(κ³-P^{Ph}N^{Bn})₂Mn(CO)(bppm)]⁺[BAR^F₄][−],^{6k} and [(κ³-P^{Ph}N^{Me}P^{Ph})Mn(CO)₃]⁺[BAR^F₄][−].²⁴ However, no κ³-PNP Mo complexes have been reported, although several κ²-PNP Mo complexes have been reported.^{8,25}

Scheme 3



A singlet at -8.2 ppm is observed in the $^{31}\text{P}\{^1\text{H}\}$ NMR spectrum of $[\text{CpMo}(\text{CO})(\kappa^3\text{-P}^{\text{Et}}\text{N}^{\text{Me}}\text{P}^{\text{Et}})]^+$ in fluorobenzene, while the phosphorus resonance of $[\text{CpMo}(\text{CO})(\kappa^3\text{-P}^{\text{Ph}}\text{N}^{\text{Me}}\text{P}^{\text{Ph}})]^+$ is a singlet at -6.3 ppm in $\text{PhBr-}d_5$. Both of these are significantly upfield-shifted compared to the corresponding κ^2 -PNP Mo hydride complexes.²⁶ ^1H , ^{31}P , and ^{13}C NMR spectra of $[\text{CpMo}(\text{CO})(\kappa^3\text{-P}^{\text{R}}\text{N}^{\text{Me}}\text{P}^{\text{R}})]^+$ (R = Et, Ph) all indicate symmetrical structures in solution. Upfield-shifted ^{31}P NMR resonances of four-membered phosphacycle rings have been reported for other κ^3 -PNP or κ^3 -P₂N₂ metal complexes, such as $[(\kappa^3\text{-P}^{\text{Ph}}\text{N}^{\text{Me}}\text{P}^{\text{Ph}})\text{Mn}(\text{CO})_3]^+$ (-3.5 ppm).²⁴ $[\text{CpMo}(\text{CO})(\kappa^3\text{-P}^{\text{Et}}\text{N}^{\text{Me}}\text{P}^{\text{Et}})]^+[\text{BARF}_4]^-$ and $[\text{CpMo}(\text{CO})(\kappa^3\text{-P}^{\text{Ph}}\text{N}^{\text{Me}}\text{P}^{\text{Ph}})]^+[\text{BARF}_4]^-$ show carbonyl stretching bands ($\tilde{\nu}_{\text{CO}}$) at 1844 and 1859 cm^{-1} , respectively, in the IR spectrum in fluorobenzene (Table 1).

Single crystals of $[\text{CpMo}(\text{CO})(\kappa^3\text{-P}^{\text{Et}}\text{N}^{\text{Me}}\text{P}^{\text{Et}})]^+[\text{BARF}_4]^-$ and $[\text{CpMo}(\text{CO})(\kappa^3\text{-P}^{\text{Ph}}\text{N}^{\text{Me}}\text{P}^{\text{Ph}})]^+[\text{BARF}_4]^- \cdot 2\text{PhF}$ were both grown by slow diffusion of pentane into fluorobenzene solutions, and were characterized by X-ray diffraction. The structures clearly show the κ^3 coordination mode of PNP ligand, two Mo–P–C–N four-membered rings and wide P–Mo–P angles (Figure 4). In the structure of $[\text{CpMo}(\text{CO})(\kappa^3\text{-P}^{\text{Et}}\text{N}^{\text{Me}}\text{P}^{\text{Et}})]^+[\text{BARF}_4]^-$, the four legs of the piano-stool geometry are irregularly positioned around Mo: the C–Mo–P angles of $81.88(5)^\circ$ and $81.68(5)^\circ$ are significantly larger than the P–Mo–N angles of $64.90(3)^\circ$ and $65.58(3)^\circ$. These results indicate that Mo–PNP coordination geometry is distorted because the flexible PNP ligand leads to a larger P–Mo–P bond angle of $123.220(16)^\circ$ to accommodate the Mo–N coordination. The P–Mo–P bond angles of known κ^2 -Mo-PNP complexes range from 74.9° to 89.7° , much smaller than the value in $[\text{CpMo}(\text{CO})(\kappa^3\text{-P}^{\text{Et}}\text{N}^{\text{Me}}\text{P}^{\text{Et}})]^+[\text{BARF}_4]^-$.^{8,25a,c,e} The Mo–N bond length is $2.3083(13)\text{ \AA}$, which falls into the range of Mo–N dative bond lengths ($2.1\text{--}2.4\text{ \AA}$) based on a search of the Cambridge Structural Database. The coordination geometry of $[\text{CpMo}(\text{CO})(\kappa^3\text{-P}^{\text{Ph}}\text{N}^{\text{Me}}\text{P}^{\text{Ph}})]^+[\text{BARF}_4]^-$ is similar to that of $[\text{CpMo}(\text{CO})(\kappa^3\text{-P}^{\text{Et}}\text{N}^{\text{Me}}\text{P}^{\text{Et}})]^+[\text{BARF}_4]^-$, and selected bond length and angles are listed in Table 4.

No reaction was observed between $[\text{CpMo}(\text{CO})(\kappa^3\text{-P}^{\text{R}}\text{N}^{\text{Me}}\text{P}^{\text{R}})]^+$ (R = Et, Ph) and H_2 (1.4 atm) in fluorobenzene at 22°C as monitored by both ^1H and ^{31}P NMR spectroscopy. The metal dihydride complex $[\text{CpMo}(\text{CO})(\kappa^2\text{-P}^{\text{R}}\text{N}^{\text{Me}}\text{P}^{\text{R}})(\text{H})_2]^+$ was not observed in the ^1H NMR spectra. (We have generated $[\text{CpMo}(\text{CO})(\kappa^2\text{-P}^{\text{Et}}\text{N}^{\text{Me}}\text{P}^{\text{Et}})(\text{H})_2]^+$ in solution by protonation of $\text{CpMo}(\text{CO})(\kappa^2\text{-P}^{\text{Et}}\text{N}^{\text{Me}}\text{P}^{\text{Et}})\text{H}$, as described in a later section.) We suggest that the Mo–N coordination is too strong to dissociate and generate a vacant site for H_2 coordination. $[\text{CpMo}(\text{CO})(\kappa^3\text{-P}^{\text{R}}\text{N}^{\text{Me}}\text{P}^{\text{R}})]^+$ reacts slowly in neat CD_3CN (3 h) to give the CD_3CN adduct $[\text{CpMo}(\text{CO})(\kappa^3\text{-P}^{\text{R}}\text{N}^{\text{Me}}\text{P}^{\text{R}})(\text{CD}_3\text{CN})]^+$, which is in sharp contrast to the rapid reaction of cationic $[\text{CpMo}(\text{CO})_2(\text{P}^{\text{R}}\text{R}_3)]^+[\text{B}(\text{C}_6\text{F}_5)_4]^-$ with acetonitrile.²² We determined the kinetics of solvolysis of $[\text{CpMo}(\text{CO})(\kappa^3\text{-P}^{\text{Et}}\text{N}^{\text{Me}}\text{P}^{\text{Et}})]^+[\text{B}(\text{C}_6\text{F}_5)_4]^-$ in MeCN using

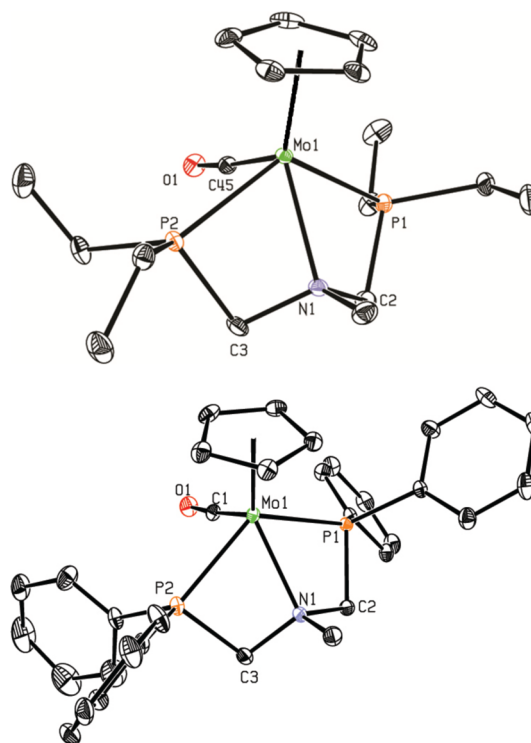


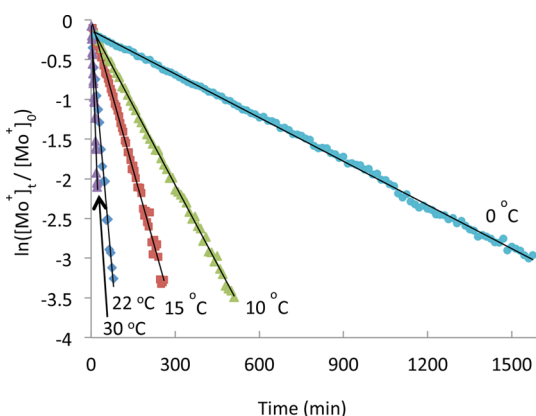
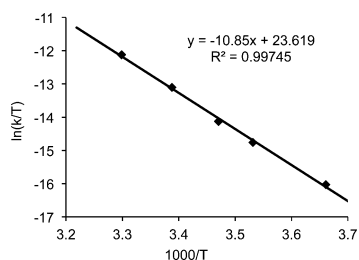
Figure 4. ORTEP drawing of $[\text{CpMo}(\text{CO})(\kappa^3\text{-P}^{\text{Et}}\text{N}^{\text{Me}}\text{P}^{\text{Et}})]^+[\text{BARF}_4]^-$ (upper) and $[\text{CpMo}(\text{CO})(\kappa^3\text{-P}^{\text{Ph}}\text{N}^{\text{Me}}\text{P}^{\text{Ph}})]^+[\text{BARF}_4]^- \cdot 2\text{PhF}$ (lower) with 30% thermal ellipsoids; hydrogen atoms are omitted for clarity. BARF_4 anions in both structures and two cocrystallized fluorobenzene molecules in $[\text{CpMo}(\text{CO})(\kappa^3\text{-P}^{\text{Ph}}\text{N}^{\text{Me}}\text{P}^{\text{Ph}})]^+[\text{BARF}_4]^- \cdot 2\text{PhF}$ are not shown.

variable temperature $^{31}\text{P}\{^1\text{H}\}$ NMR spectroscopy. The measurements show that the disappearance of the Mo complex follows pseudo-first-order kinetics (Figure 5). Rate constants were determined at five temperatures over the range $0\text{--}30^\circ\text{C}$ (Figure 6) and are linear to more than four half-lives, giving the activation parameters $\Delta H^\ddagger = 21.6 \pm 2.8\text{ kcal/mol}$, $\Delta S^\ddagger = -0.3 \pm 9.8\text{ cal/(mol K)}$, $E_a = 22.1 \pm 2.8\text{ kcal/mol}$, $\log(A) = 13.1 \pm 2.1$.

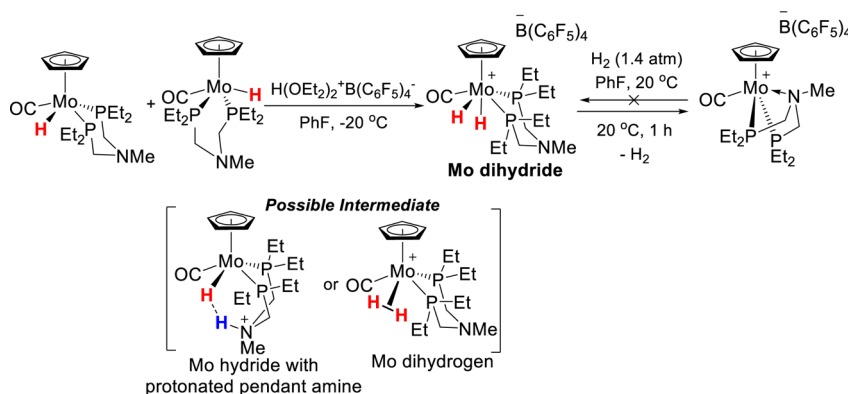
Protonation of $\text{CpMo}(\text{CO})(\text{PNP})\text{H}$ To Form $[\text{CpMo}(\text{CO})(\text{PNP})(\text{H})_2]^+$ Complexes. Since $[\text{CpMo}(\text{CO})(\kappa^3\text{-PNP})]^+$ is unreactive with H_2 , the protonation of $\text{CpMo}(\text{CO})(\text{P}^{\text{Et}}\text{N}^{\text{Me}}\text{P}^{\text{Et}})\text{H}$ was carried out to synthesize the Mo dihydride complex, $[\text{CpMo}(\text{CO})(\text{PNP})(\text{H})_2]^+$, Scheme 4. Addition of $[\text{H}(\text{OEt})_2]^+[\text{B}(\text{C}_6\text{F}_5)_4]^-$ to $\text{CpMo}(\text{CO})(\text{P}^{\text{Et}}\text{N}^{\text{Me}}\text{P}^{\text{Et}})\text{H}$ in fluorobenzene solution at -35°C affords $[\text{CpMo}(\text{CO})(\kappa^2\text{-P}^{\text{Et}}\text{N}^{\text{Me}}\text{P}^{\text{Et}})(\text{H})_2]^+[\text{B}(\text{C}_6\text{F}_5)_4]^-$ in 84% yield.²⁷ In solution, $\text{CpMo}(\text{CO})(\kappa^2\text{-P}^{\text{Et}}\text{N}^{\text{Me}}\text{P}^{\text{Et}})(\text{H})_2^+$ is stable below 0°C , but at 20°C , $[\text{CpMo}(\text{CO})(\kappa^2\text{-P}^{\text{Et}}\text{N}^{\text{Me}}\text{P}^{\text{Et}})(\text{H})_2]^+$ readily loses H_2 to generate $[\text{CpMo}(\text{CO})(\kappa^3\text{-P}^{\text{Et}}\text{N}^{\text{Me}}\text{P}^{\text{Et}})]^+$, which is stable at room temperature as a solid.

Table 4. Selected Bond Lengths (Å) and Angles (deg) for the $[\text{CpMo}(\text{CO})(\kappa^3\text{-PNP})]^+$ and $[\text{CpMo}(\text{CO})(\kappa^2\text{-PNP})(\text{H})_2]^+$ Complexes

	$[\text{CpMo}(\text{CO})(\kappa^3\text{-P}^{\text{Et}}\text{N}^{\text{Me}}\text{P}^{\text{Et}})]^+[\text{BAr}^{\text{F}}_4]^-$	$[\text{CpMo}(\text{CO})(\kappa^3\text{-P}^{\text{Ph}}\text{N}^{\text{Me}}\text{P}^{\text{Ph}})]^+[\text{BAr}^{\text{F}}_4]^- \cdot 2\text{PhF}$	$[\text{CpMo}(\text{CO})(\kappa^2\text{-P}^{\text{Et}}\text{N}^{\text{Me}}\text{P}^{\text{Et}})(\text{H})_2]^+[\text{B}(\text{C}_6\text{F}_5)_4]^-$
Mo–Cp _{centroid}	2.001	1.995	1.978
Mo–P1	2.4527(5)	2.4715(7)	2.4674(8)
Mo–P2	2.4406(5)	2.4316(6)	2.4593(9)
Mo–C _(CO)	1.9119(15)	1.927(3)	1.990(4)
Mo–N	2.3083(13)	2.295(2)	
Mo–H			1.54(4) (cis to Cp) 1.68(4) (trans to Cp)
C–O	1.1735(19)	1.173(3)	1.132(5)
P–Mo–P	123.220(16)	122.20(2)	85.23(3)
P1–Mo–N	65.58(3)	65.09(5)	
P2–Mo–N	64.90(3)	65.95(5)	

**Figure 5.** First-order plots for rate of disappearance of $[\text{CpMo}(\text{CO})(\kappa^3\text{-P}^{\text{Et}}\text{N}^{\text{Me}}\text{P}^{\text{Et}})]^+[\text{B}(\text{C}_6\text{F}_5)_4]^-$ in MeCN at five temperatures (0–30 °C). $[\text{Mo}^+] =$ concentration of $[\text{CpMo}(\text{CO})(\kappa^3\text{-P}^{\text{Et}}\text{N}^{\text{Me}}\text{P}^{\text{Et}})]^+$.**Figure 6.** Eyring plot for solvolysis of $[\text{CpMo}(\text{CO})(\kappa^3\text{-P}^{\text{Et}}\text{N}^{\text{Me}}\text{P}^{\text{Et}})]^+[\text{B}(\text{C}_6\text{F}_5)_4]^-$ in MeCN (0–30 °C).

The dihydride resonance of $[\text{CpMo}(\text{CO})(\kappa^2\text{-P}^{\text{Et}}\text{N}^{\text{Me}}\text{P}^{\text{Et}})(\text{H})_2]^+$ is a triplet at -5.33 ppm ($^2J_{\text{PH}} \cong 31$ Hz) at -40 °C (Figure S16). The coupling constant is comparable to the value found for $[\text{CpMo}(\text{CO})(\text{dppe})(\text{H})_2]^+\text{OTf}^-$ ($^2J_{\text{PH}} = 32.7$ Hz at -58 °C). Variable temperature ^1H NMR spectra in fluorobenzene/toluene- d_8 (1:1) show that $^2J_{\text{PH}}$ is temperature independent, and the two hydrides are equivalent in the range -60 to 20 °C. The T_1 relaxation time for the dihydride resonance reaches a minimum as 400 ms at -20 °C in fluorobenzene (in the range -40 to 20 °C), indicating a Mo dihydride rather than a Mo dihydrogen complex.²⁸ In the $^{31}\text{P}\{^1\text{H}\}$ NMR spectrum at -60 °C, two broad singlets are observed at 26.1 and 22.1 ppm for the inequivalent phosphines. At -30 °C the phosphine resonances broaden and show coalescence. At -20 °C the two phosphine resonances merge to a broad singlet at 24.2 ppm, indicating fluxional behavior of the PNP ligand in solution. Protonation of $\text{CpMo}(\text{CO})(\text{P}^{\text{Et}}\text{N}^{\text{Me}}\text{P}^{\text{Et}})\text{H}$ with $[\text{D}(\text{OEt}_2)_2]^+[\text{B}(\text{C}_6\text{F}_5)_4]^-$ leads to formation of $[\text{CpMo}(\text{CO})(\kappa^2\text{-P}^{\text{Et}}\text{N}^{\text{Me}}\text{P}^{\text{Et}})(\text{H})(\text{D})]^+[\text{B}(\text{C}_6\text{F}_5)_4]^-$, showing a triplet at -5.30 ppm ($^2J_{\text{PH}} = 31$ Hz) in the ^1H NMR spectrum at 20 °C. No significant $^1J_{\text{HD}}$ was observed, suggesting again that the protonated complex is Mo dihydride rather than dihydrogen complex.²⁹ The ^2D NMR spectrum shows a broad singlet at -5.00 ppm. $[\text{CpMo}(\text{CO})(\kappa^2\text{-P}^{\text{Et}}\text{N}^{\text{Me}}\text{P}^{\text{Et}})(\text{H})_2]^+$ shows a carbonyl stretching band ($\tilde{\nu}_{\text{CO}}$) at 2037 cm^{-1} in the IR spectrum in fluorobenzene, which appears at higher energy than the bands for the neutral hydride $\text{CpMo}(\text{CO})(\text{P}^{\text{Et}}\text{N}^{\text{Me}}\text{P}^{\text{Et}})\text{H}$ (1819 cm^{-1}), as expected in view of the charge and the higher formal oxidation state of Mo in the dihydride.

Scheme 4

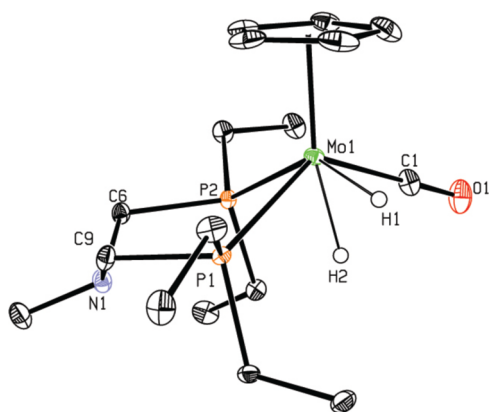


Figure 7. ORTEP drawing of $[\text{CpMo}(\text{CO})(\kappa^2\text{-P}^{\text{Et}}\text{N}^{\text{Me}}\text{P}^{\text{Et}})(\text{H})_2]^+[\text{B}(\text{C}_6\text{F}_5)_4]^-$ with 30% thermal ellipsoids and hydrogen atoms omitted for clarity, except Mo–H. $\text{B}(\text{C}_6\text{F}_5)_4$ anion is not shown.

Single crystals of $[\text{CpMo}(\text{CO})(\kappa^2\text{-P}^{\text{Et}}\text{N}^{\text{Me}}\text{P}^{\text{Et}})(\text{H})_2]^+[\text{B}(\text{C}_6\text{F}_5)_4]^-$ were grown by slow diffusion of pentane into a fluorobenzene solution at -35°C , and were analyzed by X-ray diffraction (Figure 7). Both hydrides were located on the electron density map. Selected bond distances and angles are listed in Table 4. The coordination geometry is similar to the related W dihydride $[\text{CpW}(\text{CO})_2(\text{PMe}_3)(\text{H})_2]^+\text{OTf}^-$.³⁰ One of the hydrides is *trans* to the Cp ligand, and two phosphines, the carbonyl group, and another hydride *cis* to the Cp complete the other legs of the piano-stool coordination sphere (Figure 7). The PNP ligand adopts a chair conformation. The distance of the nitrogen atom of pendant amine to the hydride *trans* to the Cp is 3.865 Å, which is too long of a distance to have any interaction.

However, when we tried to protonate $\text{CpMo}(\text{CO})(\text{P}^{\text{Ph}}\text{N}^{\text{Me}}\text{P}^{\text{Ph}})\text{H}$ with $[\text{H}(\text{OEt})_2]^+[\text{B}(\text{C}_6\text{F}_5)_4]^-$ in fluorobenzene solution at low temperature, $[\text{CpMo}(\text{CO})(\kappa^2\text{-P}^{\text{Ph}}\text{N}^{\text{Me}}\text{P}^{\text{Ph}})(\text{H})_2]^+$ could not be observed or isolated. We observed gas evolution (presumably H_2) in seconds, even at -20°C . Subsequent ^1H and ^{31}P NMR spectra identified the product as $[\text{CpMo}(\text{CO})(\kappa^3\text{-P}^{\text{Ph}}\text{N}^{\text{Me}}\text{P}^{\text{Ph}})]^+$. Protonation at lower temperature in fluorobenzene did not proceed, probably due to low solubility of $\text{CpMo}(\text{CO})(\text{P}^{\text{Ph}}\text{N}^{\text{Me}}\text{P}^{\text{Ph}})\text{H}$.

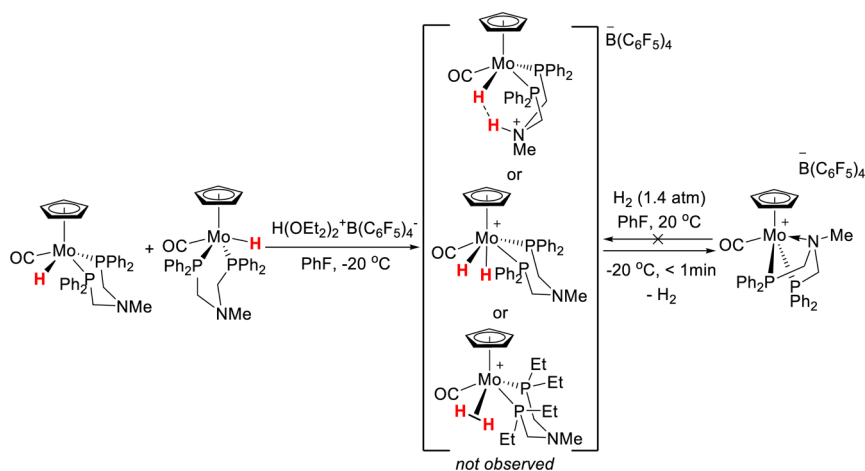
The possible initial protonation of the Mo–PNP hydride complexes might occur at the pendant amine to give a Mo

hydride complex bearing a protonated pendant amine, followed by intramolecular proton transfer to Mo leading to a Mo dihydride complex. Alternatively, protonation of Mo hydride could afford a cationic Mo dihydrogen complex,^{29a,b,g} and then oxidative addition of the dihydrogen ligand would give the Mo dihydride complex. However, neither a Mo hydride complex bearing a protonated pendant amine nor a Mo dihydrogen complex was observed by ^1H NMR spectroscopy. We suggest that the pendant amine is not as basic as the Mo center in $[\text{CpMo}(\text{CO})(\kappa^2\text{-P}^{\text{Et}}\text{N}^{\text{Me}}\text{P}^{\text{Et}})(\text{H})_2]^+$, probably because the alkyl substituted $\text{P}^{\text{Et}}\text{N}^{\text{Me}}\text{P}^{\text{Et}}$ ligand makes Mo center more electron-rich and basic.

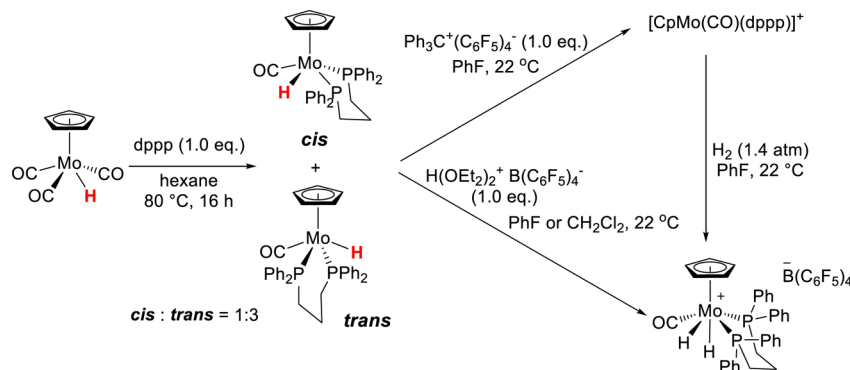
The instability of $[\text{CpMo}(\text{CO})(\kappa^2\text{-PNP})(\text{H})_2]^+$ is likely due to a low activation barrier for H_2 dissociation and the driving force to form the thermodynamically stable $[\text{CpMo}(\text{CO})(\kappa^3\text{-PNP})]^+$ complex. In the case of protonation of $\text{CpMo}(\text{CO})(\text{P}^{\text{Ph}}\text{N}^{\text{Me}}\text{P}^{\text{Ph}})\text{H}$, even though the more electron-deficient phenyl groups on the PNP ligand make the Mo center a better hydride acceptor, the driving force to form the tuck-in Mo–N bond is also likely stronger, leading to the formation of $[\text{CpMo}(\text{CO})(\kappa^3\text{-P}^{\text{Ph}}\text{N}^{\text{Me}}\text{P}^{\text{Ph}})]^+$. Though we propose the Mo dihydride species $[\text{CpMo}(\text{CO})(\kappa^2\text{-P}^{\text{Ph}}\text{N}^{\text{Me}}\text{P}^{\text{Ph}})(\text{H})_2]^+$ might be a possible intermediate, formation of Mo hydride complex bearing a protonated pendant amine cannot be ruled out (Scheme 5).

Synthesis and Protonation of $\text{CpMo}(\text{CO})(\text{dppp})\text{H}$ Complexes without a Pendant Amine. Complexes with a dppp ligand [dppp = 1,3-bis(diphenylphosphino)propane] were prepared to provide a comparison to the PNP complexes described above that contain pendant amines (Scheme 6). The diphosphine dppp was chosen since it has the same number of atoms in the linkage connecting the two phosphines. The reaction of $\text{CpMo}(\text{CO})_3\text{H}$ with dppp is much slower than the reaction with the PNP ligand. Ligand substitution of $\text{CpMo}(\text{CO})_3\text{H}$ with dppp was complete after 16 h at 80°C in hexane solution, and $\text{CpMo}(\text{CO})(\text{dppp})\text{H}$ was isolated in 56% yield as a 1:3 mixture of *cis*- and *trans*-isomers, based on ^1H and ^{31}P NMR spectra. This isomer ratio contrasts with our previous result on $\text{CpMo}(\text{CO})(\text{dppe})\text{H}$, which was isolated only as the *cis*-isomer.⁵ The selectivity favoring the *trans*-isomer as the major product is similar to the formation of $\text{CpMo}(\text{CO})(\text{P}^{\text{Ph}}\text{N}^{\text{Me}}\text{P}^{\text{Ph}})\text{H}$, which is not surprising since dppp has similar electronic characteristics as $\text{P}^{\text{Ph}}\text{N}^{\text{Me}}\text{P}^{\text{Ph}}$. The metal hydride complex $\text{CpMo}(\text{CO})(\text{dppe})\text{H}$ was synthesized by hydride reduction of $\text{CpMo}(\text{CO})(\text{dppe})\text{Cl}$ instead of direct ligand

Scheme 5



Scheme 6



substitution of $\text{CpMo(CO)}_3\text{H}$ with dppe ,⁵ which indicates that an additional CH_2 in the linkage between two phosphines makes the substitution of CO by phosphine more facile, probably due to the larger bite angle during the second substitution.

The NMR characteristics of CpMo(CO)(dppp)H are very similar to those of $\text{CpMo(CO)(P}^{\text{Ph}}\text{N}^{\text{Me}}\text{P}^{\text{Ph}}\text{)H}$. The hydride resonances appear as triplets at -5.56 ppm ($^2J_{\text{HP}} = 41$ Hz, *cis*) and -6.82 ppm ($^2J_{\text{HP}} = 73$ Hz, *trans*) in the ^1H NMR spectrum at 20 °C. The triplet for the *cis*-isomer transforms to a doublet of doublets ($^2J_{\text{HP}} = 63$ Hz; $^2J_{\text{HP}} = 15$ Hz) at -40 °C, and the triplet for the *trans*-isomer does not change. The phosphorus resonances show a singlet at 72.5 ppm for the *trans*-isomer and a broad singlet at 51.2 ppm for the *cis*-isomer in the $^{31}\text{P}\{^1\text{H}\}$ NMR spectrum. This broad singlet transforms into two doublets at 53.5 and 49.0 ppm ($^2J_{\text{PP}} = 65$ Hz) at -40 °C. See Supporting Information for ^1H and ^{31}P NMR spectra at 20 °C and -40 °C.

Single crystals of *trans*- CpMo(CO)(dppp)H were grown by cooling a hot hexane solution, and were analyzed by X-ray diffraction (Figure 8, left). Selected bond distances and angles are provided in Table 5. The four-legged piano-stool coordination geometry of *trans*- CpMo(CO)(dppp)H is very similar to that of *trans*- $\text{CpMo(CO)(P}^{\text{Ph}}\text{N}^{\text{Me}}\text{P}^{\text{Ph}}\text{)H}$. The P–Mo–P bond angle of $99.12(2)^\circ$ is slightly larger than the value of $97.54(17)^\circ$ in *trans*- $\text{CpMo(CO)(P}^{\text{Ph}}\text{N}^{\text{Me}}\text{P}^{\text{Ph}}\text{)H}$.

Reaction of CpMo(CO)(dppp)H with $[\text{Ph}_3\text{C}]^+[\text{B}(\text{C}_6\text{F}_5)_4]^-$ in fluorobenzene gives a mixture of products, as indicated by several peaks in the ^{31}P NMR spectrum. Plausible products include a cationic complex with an agostic C–H bond or a complex with one $\eta^2\text{-C}\equiv\text{C}$ coordination of Mo with the $\text{C}\equiv\text{C}$ of a Ph ring. The metal dihydride $[\text{CpMo(CO)(dppp)(H)}_2]^+[\text{B}(\text{C}_6\text{F}_5)_4]^-$ species is also observed in approximately 20% yield. The metal dihydride likely results from protonation of CpMo(CO)(dppp)H by the radical cation $[\text{CpMo(CO)(dppp)H}]^{+\bullet}$ that results from one-electron oxidation of CpMo(CO)(dppp)H by $[\text{Ph}_3\text{C}]^+$. One-electron oxidation of metal hydrides has been shown to increase their acidity, by as much as $14\text{--}26$ pK_a units.^{17,31} Similar proton transfers to give metal dihydrides or metal hydride bearing a protonated pendant amine have been reported.^{5,24} The mixture of cationic complexes resulting from hydride abstraction was found to react with H_2 to give $[\text{CpMo(CO)(dppp)(H)}_2]^+[\text{B}(\text{C}_6\text{F}_5)_4]^-$. Protonation of CpMo(CO)(dppp)H with $[\text{H}(\text{OEt}_2)_2]^+[\text{B}(\text{C}_6\text{F}_5)_4]^-$ in fluorobenzene or CH_2Cl_2 also leads to formation of the dihydride complex $[\text{CpMo(CO)(dppp)(H)}_2]^+[\text{B}(\text{C}_6\text{F}_5)_4]^-$ (Scheme 6). $[\text{CpMo(CO)(dppp)(H)}_2]^+$ slowly decomposes to give a mixture of unidentified products under

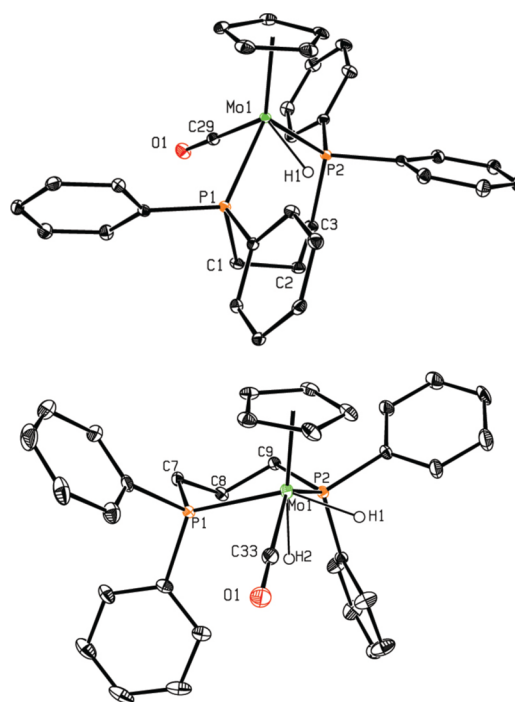


Figure 8. ORTEP drawing of *trans*- CpMo(CO)(dppp)H (upper) and $[\text{CpMo(CO)(dppp)(H)}_2]^+[\text{B}(\text{C}_6\text{F}_5)_4]^- \cdot 2\text{CH}_2\text{Cl}_2$ (lower) with 30% thermal ellipsoids and hydrogen atoms omitted for clarity, except Mo–H. $\text{B}(\text{C}_6\text{F}_5)_4$ anion and two cocrystallized CH_2Cl_2 molecules in $[\text{CpMo(CO)(dppp)(H)}_2]^+[\text{B}(\text{C}_6\text{F}_5)_4]^- \cdot 2\text{CH}_2\text{Cl}_2$ are not shown.

Table 5. Selected Bond Lengths (Å) and Angles (deg) for the *trans*- CpMo(CO)(dppp)H and $[\text{CpMo(CO)(dppp)(H)}_2]^+[\text{B}(\text{C}_6\text{F}_5)_4]^- \cdot 2\text{CH}_2\text{Cl}_2$ Complexes

	<i>trans</i> - CpMo(CO)(dppp)H	$[\text{CpMo(CO)(dppp)(H)}_2]^+[\text{B}(\text{C}_6\text{F}_5)_4]^- \cdot 2\text{CH}_2\text{Cl}_2$
Mo–P1	2.3737(6)	2.4735(10)
Mo–P2	2.3372(6)	2.4826(10)
Mo–C _(CO)	1.919(2)	1.966(4)
P–Mo–P	99.21(2)	88.72(3)

an N_2 atmosphere in solution or under vacuum, but it is stable under an H_2 atmosphere in solution.

The dihydride complex $[\text{CpMo(CO)(dppp)(H)}_2]^+$ exhibits a triplet for the dihydride resonance at -3.30 ppm ($^2J_{\text{PH}} \cong 31$ Hz) at 20 °C in the ^1H NMR spectrum. The coupling constant is very similar to that of $[\text{CpMo(CO)(}\kappa^2\text{-P}^{\text{Et}}\text{N}^{\text{Me}}\text{P}^{\text{Et}}\text{)(H)}_2]^+[\text{B}(\text{C}_6\text{F}_5)_4]^-$ ($^2J_{\text{PH}} = 31$ Hz at -40 °C) and $[\text{CpMo(CO)(dppe)-}$

(H)₂]⁺[OTf][−] (²J_{PH} = 32.7 Hz at −58 °C). The triplet for the hydride in ¹H NMR spectrum transforms to a doublet of doublets (²J_{HP} ≈ 33 Hz; ²J_{HP′} ≈ 24 Hz) at −70 °C in CD₂Cl₂. T₁ (min) for the dihydride resonance reaches its minimum as 313 ms at 0 °C in fluorobenzene, suggesting its dihydride nature rather than a dihydrogen complex. In the ³¹P{¹H} NMR spectrum at −80 °C, two doublets are observed at 30.2 and 27.4 ppm, which broaden and transform to two broad singlets at −50 °C. At higher temperature (−20 °C) the two phosphine resonances coalesce, merging to a broad singlet at 28.2 ppm.

Single crystals of [CpMo(CO)(dppp)(H)₂]⁺[B(C₆F₅)₄][−] · 2CH₂Cl₂ were grown by slow diffusion of pentane into a dichloromethane solution at −35 °C, and were analyzed by X-ray diffraction (Figure 8, right). Both hydrides were located on the electron density map. Selected bond distances and angles are listed in Table 5. The distorted octahedral coordination geometry of the Mo cation is very similar to its analogue [CpMo(CO)(κ²-P^{Et}N^{Me}P^{Et})(H)₂]⁺ and to the related W dihydride [CpW(CO)₂(PMe₃)(H)₂]⁺OTf[−],³⁰ with one of the hydrides being *trans* to the Cp ligand (Figure 8, right).

The role of the pendant amine is apparent. While the Mo diphosphine dihydride complexes [CpMo(CO)(κ²-PNP)-(H)₂]⁺ and [CpMo(CO)(dppp)(H)₂]⁺ are both unstable and release H₂ under an N₂ atmosphere in solution or under vacuum, [CpMo(CO)(κ²-PNP)(H)₂]⁺ shows faster decomposition because of the driving force provided by formation of the Mo–N bond. The presence of an H₂ atmosphere does not prevent decomposition. Without a pendant amine, no tuck-in κ³-complex is possible, and [CpMo(CO)(dppp)(H)₂]⁺ decomposes more slowly, and is stable under an H₂ atmosphere. Thus, in this Mo diphosphine system, the pendant amine is not basic enough to promote an intramolecular proton relay from the Mo center. Instead, the pendant amine has a strong driving force to form a stable tuck-in κ³-complex, which prevents the cationic [CpMo(CO)(κ³-PNP)]⁺ complexes from reacting with H₂. These results suggest Mo-PNP complexes are less attractive for further studies aimed at heterolytic H₂ cleavage. Further design and modification of this Mo diphosphine system for heterolytic H₂ cleavage will need to prevent the strong tuck-in N-coordination, and tune the acidity of Mo center and basicity of the pendant amine.

CONCLUSIONS

We report the synthesis, spectroscopic characterization, X-ray single crystal structures, electrochemical oxidation, hydride abstraction, and protonation studies of CpMo(CO)(PNP)H complexes as Mo diphosphine complexes bearing pendant amine. “Tuck-in” [CpMo(CO)(κ³-PNP)]⁺ complexes as products of hydride abstraction showed a bound amine, and the complex did not react with H₂. Kinetic measurement of solvolysis of [CpMo(CO)(κ³-P^{Et}N^{Me}P^{Et})]⁺ in MeCN gave pseudo-first-order kinetics (ΔH[‡] = 21.6 ± 2.8 kcal/mol, ΔS[‡] = −0.3 ± 9.8 cal/(mol K), E_a = 22.1 ± 2.8 kcal/mol), and provided an estimated upper limit of the energy of the Mo–N bond. [CpMo(CO)(κ²-P^{Et}N^{Me}P^{Et})(H)₂]⁺ was prepared by protonation of CpMo(CO)(P^{Et}N^{Me}P^{Et})H, and loses H₂ to generate [CpMo(CO)(κ³-P^{Et}N^{Me}P^{Et})]⁺. The pendant amine is not sufficiently basic to deprotonate the Mo dihydride; instead, it plays a key role in H₂ elimination and accelerates this process by formation of a Mo–N dative bond. In the case of [CpMo(CO)(dppp)(H)₂]⁺, with no pendant amine, hydrogen elimination was suppressed in the presence of an H₂ atmosphere.

EXPERIMENTAL SECTION

General Methods. All manipulations were carried out under N₂ using standard Schlenk and inert atmosphere glovebox techniques. Dichloromethane, diethyl ether, THF, fluorobenzene, pentane, and hexane were purified by passage through neutral alumina, using an Innovative Technology, Inc., Pure Solv solvent purification system. Deuterated solvents (Cambridge Isotope Laboratories, 99.5% D or greater) were dried as follows: C₆D₆ was dried by stirring over CaH₂ and was vacuum distilled; CD₃CN was dried over P₂O₅ and vacuum distilled. [Ph₃C]⁺[B(C₆F₅)₄][−] and [Ph₃C]⁺[BAR^F₄][−] were purified twice by dissolution in CH₂Cl₂ and subsequent precipitation with hexanes.³² [H(OEt)₂]⁺[B(C₆F₅)₄][−] was prepared following a previously reported procedure.³³ P^{Et}N^{Me}P^{Et} and P^{Ph}N^{Me}P^{Ph} were prepared as described in the literature.^{6d,8,25e} CpMo(CO)₃H was prepared as described in the literature³⁴ and purified by sublimation³⁵ under dynamic vacuum at 50–80 °C, giving pale yellow crystals in ca. 90% yield.

Instrumentation. Electrochemical measurements were performed using a CH Instruments potentiostat equipped with a standard three-electrode cell consisting of a 4 mL disposable glass vial fitted with a polyethylene cap having openings sized to closely accept each electrode. For each experiment, the cell was assembled and used within the glovebox, with electrodes connected to the potentiostat via RF-shielded cables fed through the glovebox wall. The working electrode (1 mm PEEK-encased glassy carbon, Cypress Systems EE040) was polished using alumina (BAS CF-1050, dried at 150 °C under vacuum) suspended in acetonitrile, and then rinsed with neat acetonitrile. A glassy carbon rod (Structure Probe, Inc.) was used as the counterelectrode, and a silver chloride coated silver wire suspended in a solution of 0.2 M [Bu₄N]⁺[PF₆][−] in acetonitrile and separated from the analyte solution by a porous Teflon tip (CH Instruments 112) was used as the pseudoreference electrode. Potentials are reported versus the Cp₂Fe^{•+/0} couple, and were determined versus cobaltocene (E° = −1.33 V vs Cp₂Fe^{•+/0}).

Organometallic samples for NMR spectroscopic measurements were prepared in a glovebox using J. Young NMR tubes (Wilmad 528-JY). ¹H, ³¹P, ¹³C, ¹⁵N NMR spectra as well as 2D NMR spectra were recorded on a Varian 500 MHz spectrometer at room temperature, unless otherwise noted. For spectra recorded in (protio)-fluorobenzene, ca. 10% C₆D₆ was added for the purpose of locking and shimming. ¹H NMR spectra recorded in this manner were referenced by centering the lowest-field multiplet of fluorobenzene at 7.05 ppm; the latter chemical shift was determined from a separately run ¹H NMR spectrum of Si(CH₃)₄ (≡ 0 ppm) in the same solvent mixture, under the same conditions. Spectra of other nuclei were referenced with respect to a referenced ¹H NMR spectrum with the use of Varian's *mref* command; ¹³C, ³¹P, ¹⁹F, and ¹⁵N shifts thus obtained are relative to Si(CH₃)₄, 85% aq H₃PO₄, CFCl₃, and CH₃NO₂ (all at 0 ppm), respectively. Solution IR spectra were recorded in absorbance mode using a Nicolet iS10 FTIR spectrometer with demountable sealed liquid CaF₂ cells (International Crystal Laboratories). Solid state IR spectra were run as Nujol mulls, prepared by rubbing ca. 2 mg of the analyte and a drop of Nujol between two CaF₂ plates. Elemental analyses were performed by Atlantic Microlab (Norcross, GA).

Crystallography. A microscope was used to identify suitable crystals of the same habit. Each crystal was coated in Paratone, affixed to a micromount, and placed under streaming nitrogen (100 K) on a Bruker KAPPA APEX II CCD diffractometer with 0.71073 Å Mo Kα radiation. Space groups were determined on the basis of systematic absences and intensity statistics. The structures were solved by direct methods and refined by full-matrix least-squares refinement on F². Anisotropic displacement parameters were determined for all non-hydrogen atoms. Hydrogen atoms were placed at idealized positions and refined with fixed isotropic displacement parameters, with the exception of the Mo-bonded hydrogens, which were located on the electron density map and isotropically refined. In the X-ray crystal structure of CpMo(CO)(dppp)H, the residue with maximum density causes an B-level alert in the checkcif report, which is supposed to be

the Mo atom of another disordered complex. Upon releasing 50 more Q peaks, two corresponding phosphorus atoms and two carbon linkers could be found, but the weights of them are all very light. The other part of the disordered molecule could not be found. Further refinement is not necessary since it will not significantly improve the quality of the structure.

The following programs were used: SAINT-Plus version 6.63³⁶ for data reduction; SADABS³⁷ for absorption correction; SHELXS-97 and SHELXL-2013³⁸ for structure solution and refinement, respectively; Ortep-3 (version 2.02) for Windows³⁹ for graphics. OLEX2⁴⁰ was used as the graphical user interface in which structure solution and refinement were performed. Crystal data and information about data collection and refinement are listed in Supporting Information.

Synthesis of CpMo(CO)(κ^2 -P^{Et}N^{Me}P^{Et})H. The P^{Et}N^{Me}P^{Et} ligand (Et₂PCH₂NMeCH₂PEt₂, 85.0 mg, 0.20 mmol) and CpMo(CO)₃H (54.2 mg, 0.22 mmol) were dissolved in hexane (5 mL), and the orange solution was stirred at 80 °C for 4 h to give a light yellow solution. The solution was filtered, and the volatiles were concentrated under vacuum to about 2 mL. The concentrated solution was allowed to evaporate at room temperature overnight to crystallize the product, giving light yellow block crystals, which were dried under vacuum and washed with cold pentane (−20 °C) twice. Several of the blocks were found suitable for X-ray diffraction. Combined yield for *cis* + *trans* isomers: 59.5 mg (0.14 mmol, 70%). ¹H NMR (toluene-*d*₈, 500 MHz, 233 K): δ 5.05 (s, 5H, Cp, *trans*), 4.66 (s, 5H, Cp, *cis*), 2.44 (dd, ²J_{HP} = 12.2, ²J_{HH} = 9.5 Hz, 1H, PCH₂N, *cis* + *trans*), 2.27 (dd, ²J_{HP} = 11.9, ²J_{HH} = 8.9 Hz, 1H, PCH₂N, *cis* + *trans*), 2.14 (m, 1H, PCH₂N, *cis* + *trans*), 1.86 (s, 3H, NCH₃, *cis* + *trans*), 1.70–1.58 (m, 2H, CH₂CH₃, *cis* + *trans*), 1.51 (dd, ²J_{HP} = 12.4, ⁴J_{HH} = 2.9 Hz, 1H, PCH₂N, *cis* + *trans*), 1.45–1.37 (m, 2H, CH₂CH₃, *cis* + *trans*), 1.34–1.18 (m, 4H, CH₂CH₃, *cis* + *trans*), 1.00–0.87 (m, 6H, CH₂CH₃, *cis* + *trans*), 0.81 (td, ³J_{HP} = 13.6, ³J_{HH} = 7.3 Hz, 3H, CH₂CH₃, *cis* + *trans*), 0.69 (td, ³J_{HP} = 13.6, ³J_{HH} = 7.5 Hz, 3H, CH₂CH₃, *cis* + *trans*), −7.19 (dd, ²J_{HP} = 65.9, ²J_{HP'} = 17.4 Hz, 1H, Mo–H, *cis*), −8.08 (t, ²J_{HP} = 67.4 Hz, 1H, Mo–H, *trans*). ¹³C{¹H} NMR (C₆D₆, 125 MHz, 293 K): δ 250.98 (t, ²J_{CP} = 26.7 Hz, CO, *trans*), 243.59 (t, ²J_{CP} = 13.2 Hz, CO, *cis*), 85.59 (s, Cp, *trans*), 84.38 (s, Cp, *trans*), 61.75 (d, ¹J_{CP} = 4.7 Hz, PCH₂N, *trans*), 61.29 (d, ¹J_{CP} = 4.5 Hz, PCH₂N, *trans*), 59.76 (br s, PCH₂N, *cis*), 52.09 (t, ³J_{CP} = 10.1 Hz, NCH₃, *cis*), 50.57 (t, ³J_{CP} = 13.5 Hz, NCH₃, *trans*), 29.95–29.44 (m, CH₂CH₃, *trans*), 24.25 (br s, CH₂CH₃, *cis*), 23.02 (dt, ¹J_{CP} = 12.8, ³J_{CP} = 8.2 Hz, CH₂CH₃, *trans*), 9.42 (s, CH₂CH₃, *trans*), 8.36 (s, CH₂CH₃, *trans*), 7.81 (br s, CH₂CH₃, *cis*), 7.49 (br s, CH₂CH₃, *cis*). ³¹P{¹H} NMR (toluene-*d*₈, 202 MHz, 293 K): δ 70.5 (s, *trans*), 43.4 (br s, *cis*). ³¹P{¹H} NMR (toluene-*d*₈, 202 MHz, 233 K): δ 70.7 (s, *trans*), 44.5 (d, ²J_{PP} = 71.0 Hz, *cis*), 42.5 (d, ²J_{PP} = 71.0 Hz, *cis*). IR (hexanes): major (*cis*) isomer at $\tilde{\nu}_{\text{CO}}$ 1844 cm^{−1}; minor (*trans*) isomer at $\tilde{\nu}_{\text{CO}}$ 1813 cm^{−1}. IR (fluorobenzene): $\tilde{\nu}_{\text{CO}}$ 1819 cm^{−1} (br). Anal. Calcd for C₁₇H₃₃MoNOP₂: C, 48.00; H, 7.82; N, 3.29. Found: C, 48.09; H, 7.78; N, 3.46.

Synthesis of CpMo(CO)(κ^2 -P^{Ph}N^{Me}P^{Ph})H. CpMo(CO)₃H (54.2 mg, 0.22 mmol) was dissolved in hexane (10 mL), and the P^{Ph}N^{Me}P^{Ph} ligand (Ph₂PCH₂NMeCH₂PPh₂, 123.0 mg, 0.20 mmol) was added to the solution. The suspension was stirred at 80 °C for 4 h to give a light yellow suspension. The suspension was filtered, and the yellow solids were washed with hexane (2 × 2 mL). The solids were dissolved in 2 mL of fluorobenzene and hexane (1:1), and the solution was allowed to evaporate at room temperature overnight to give light yellow block crystals, which were dried under vacuum. Several of the blocks were found to be suitable for X-ray diffraction. Combined yield for *cis* + *trans* isomers: 77.4 mg (0.126 mmol, 63%, *cis*: *trans* = 1:2). ¹H NMR (THF-*d*₈: CD₂Cl₂ = 5:1, 500 MHz, 293 K): δ 7.73 (t, ³J_{HH} = 6.9 Hz, 4H, C₆H₅, *cis*), 7.58 (t, ³J_{HH} = 7.7 Hz, 4H, C₆H₅, *trans*), 7.46–7.39 (m, 2H, C₆H₅, *cis* + *trans*), 7.38–7.32 (m, 4H, C₆H₅, *cis* + *trans*), 7.26–7.15 (m, 10H, C₆H₅, *cis* + *trans*), 5.00 (s, 5H, Cp, *trans*), 4.51 (s, 5H, Cp, *cis*), 3.89 (t, ²J_{HP} = 13.1 Hz, 2H, PCH₂N, *trans*), 3.52 (d, ²J_{HP} = 12.9 Hz, 2H, PCH₂N, *cis*), 3.12 (d, ²J_{HP} = 12.8 Hz, 2H, PCH₂N, *cis*), 2.72 (dd, ²J_{HP} = 13.1 Hz, ²J_{HH} = 8.9 Hz, 2H, PCH₂N, *trans*), 2.60 (s, 3H, NCH₃, *trans*), 2.36 (s, 3H, NCH₃, *cis*), −6.00 (t, ²J_{HP} = 41.2 Hz, 1H, Mo–H, *cis*), −6.78 ppm (t, ²J_{HP} = 70.0 Hz, 1H, Mo–H, *trans*). ¹³C{¹H} NMR (THF-*d*₈: CD₂Cl₂ = 5:1, 126 MHz, 293 K): δ 246.60

(t, ²J_{CP} = 27.1 Hz, CO, *trans*), 241.37 (t, ²J_{CP} = 13.2 Hz, CO, *cis*), 149.04 (dd, ¹J_{CP} = 44.7, ³J_{CP} = 6.1 Hz, C₆H₅, *trans*), 143.81 (t, ¹J_{CP} = 17.5 Hz, C₆H₅, *cis*), 138.45 (dt, ¹J_{CP} = 19.5, ³J_{CP} = 10.3 Hz, C₆H₅, *cis*), 133.49 (t, ²J_{CP} = 5.4 Hz, C₆H₅, *trans*), 132.65 (t, ²J_{CP} = 5.0 Hz, C₆H₅, *cis*), 131.21 (t, ²J_{CP} = 4.8 Hz, C₆H₅, *cis*), 130.27 (t, ²J_{CP} = 4.2 Hz, C₆H₅, *trans*), 128.95 (s, C₆H₅, *trans*), 128.28 (s, C₆H₅, *cis*), 127.78 (s, C₆H₅, *cis*), 127.65 (s, C₆H₅, *trans*), 127.40 (t, ²J_{CP} = 4.1 Hz, C₆H₅, *trans*), 127.31 (t, ²J_{CP} = 4.1 Hz, C₆H₅, *trans*), 127.21 (t, ²J_{CP} = 4.5 Hz, C₆H₅, *cis*), 127.16 (t, ²J_{CP} = 4.5 Hz, C₆H₅, *cis*), 88.45 (s, Cp, *trans*), 86.65 (s, Cp, *cis*), 64.38 (d, ¹J_{CP} = 6.1 Hz, PCH₂N, *cis*), 63.88 (d, ¹J_{CP} = 6.3 Hz, PCH₂N, *cis*), 61.45 (t, ¹J_{CP} = 18.3 Hz, PCH₂N, *trans*), 50.98 (t, ³J_{CP} = 11.6 Hz, NCH₃, *cis*), 49.94 ppm (t, ³J_{CP} = 14.3 Hz, NCH₃, *trans*). ³¹P{¹H} NMR (toluene-*d*₈, 202 MHz, 293 K): δ 74.1 (s, *trans*), 51.1 ppm (br s, *cis*). ³¹P{¹H} NMR (toluene-*d*₈, 202 MHz, 213 K): δ 73.4 (s, *trans*), 51.6 (d, ²J_{PP} = 51.9 Hz, *cis*), 49.5 ppm (d, ²J_{PP} = 61.3 Hz, *cis*). IR (fluorobenzene): $\tilde{\nu}_{\text{CO}}$ 1810 cm^{−1}. IR (CH₂Cl₂): $\tilde{\nu}_{\text{CO}}$ 1804 cm^{−1}. Anal. Calcd for C₃₃H₃₃MoNOP₂: C, 64.18; H, 5.39; N, 2.27. Found: C, 64.12; H, 5.36; N, 2.32.

Synthesis of [CpMo(CO)(κ^2 -P^{Et}N^{Me}P^{Et})]⁺[A][−]: (A = B(C₆F₅)₄ or BAR^F₄[−]). A solution of CpMo(CO)(κ^2 -P^{Et}N^{Me}P^{Et})H (8.5 mg, 20 μ mol) in fluorobenzene (0.5 mL) was added to a solution of [Ph₃C]⁺[B(C₆F₅)₄][−] (18.4 mg, 20 μ mol) in fluorobenzene (0.5 mL) at room temperature, resulting in a color change from yellow to orange. The solution was layered with pentane (2 mL). Yield: 22.1 mg (17.2 μ mol, 86%).

When [Ph₃C]⁺[BAR^F₄][−] (22.1 mg, 20 μ mol) was used instead of [Ph₃C]⁺[B(C₆F₅)₄][−], [CpMo(CO)(κ^2 -P^{Et}N^{Me}P^{Et})]⁺[BAR^F₄][−] was synthesized in 74% isolated yield (19.2 mg) using the same procedure. Slow diffusion of pentane into the fluorobenzene solution overnight at room temperature gave the product as well-shaped yellow blocks (many of them suitable for X-ray diffraction).

[CpMo(CO)(κ^2 -P^{Et}N^{Me}P^{Et})]⁺[B(C₆F₅)₄][−]. ¹H NMR (fluorobenzene +10% C₆D₆, 500 MHz, 233 K): δ 4.71 (s, 5H, Cp), 4.19 (dd, ²J_{HP} = 14.8, ²J_{HH} = 6.1 Hz, 2H, PCH₂N), 3.93 (dt, ²J_{HP} = 14.8 Hz, ²J_{HH} = 3.5 Hz, 2H, PCH₂N), 2.11 (s, 3H, NCH₃), 1.92–1.82 (m, 2H, CH₂CH₃), 1.82–1.68 (m, 2H, CH₂CH₃), 1.39–1.21 (m, 2H, CH₂CH₃), 1.17–0.99 (m, 2H, CH₂CH₃), 0.75 (dt, ³J_{HP} = 17.9, ³J_{HH} = 7.6 Hz, 6H, CH₂CH₃), 0.65 ppm (dt, ³J_{HP} = 14.9, ³J_{HH} = 7.5 Hz, 6H, CH₂CH₃). ¹³C{¹H} NMR (C₆D₅Br, 125 MHz, 293 K): δ 244.54 (t, ²J_{CP} = 23.4 Hz, CO), 90.26 (s, Cp), 78.10 (dd, ¹J_{CP} = 37.0, ³J_{CP} = 14.7 Hz, PCH₂CH₃), 59.50 (s, NCH₃), 22.16 (d, ¹J_{CP} = 12.8 Hz, CH₂CH₃), 17.60 (d, ¹J_{CP} = 29.8 Hz, CH₂CH₃), 7.61 (s, CH₂CH₃), 7.50 ppm (dd, ²J_{CP} = 3.7, 2.9 Hz, CH₂CH₃). For B(C₆F₅)₄[−], doublets (¹J_{CF} ≈ 242 Hz) of multiplets are observed at δ 148.6, 138.5, and 136.6 ppm; quaternary C most likely obscured by fluorobenzene resonance. ³¹P{¹H} NMR (fluorobenzene +10% C₆D₆, 202 MHz, 233 K): δ −8.2 ppm (s). IR (fluorobenzene): $\tilde{\nu}_{\text{CO}}$ 1844 cm^{−1}. Anal. Calcd for C₄₉H₄₄BF₂₄MoNOP₂: C, 45.71; H, 3.44; N, 1.09. Found: C, 45.94; H, 3.32; N, 1.11.

Synthesis of [CpMo(CO)(κ^2 -P^{Et}N^{Me}P^{Et})(N≡CCD₃)]⁺[B(C₆F₅)₄][−]. The CD₃CN adduct was obtained upon dissolution of [CpMo(CO)(κ^2 -P^{Et}N^{Me}P^{Et})]⁺[B(C₆F₅)₄][−] in neat CD₃CN. The reaction was monitored by ¹H and ³¹P NMR spectroscopy. After 3 h, the reaction was complete, and the CD₃CN adduct was formed as sole product observed by NMR. ¹H NMR (CD₃CN, 500 MHz, 293 K): δ 5.26 (t, ³J_{HP} = 1.7 Hz, 5H, Cp), 3.28 (t, ²J_{HP} = 12.5 Hz, 1H, PCH₂N), 3.25 (t, ²J_{HP} = 12.5 Hz, 1H, PCH₂N), 2.68 (dd, ²J_{HP} = 13.2, ²J_{HH} = 5.8 Hz, 1H, PCH₂N), 2.50 (t, ²J_{HP} = 1.1 Hz, 3H, PCH₂N), 2.45 (d, ²J_{HP} = 2.5 Hz, 1H, PCH₂CH₃), 2.44–2.36 (m, 1H, PCH₂CH₃), 2.24 (dd, ²J_{HP} = 13.3, ³J_{HH} = 6.4 Hz, 1H, PCH₂CH₃), 2.19–2.12 (m, 1H, PCH₂CH₃), 2.00 (dd, ²J_{HP} = 14.9, ³J_{HH} = 7.5 Hz, 2H, PCH₂CH₃), 1.94–1.81 (m, 2H, PCH₂CH₃), 1.26–1.05 (m, 12H, PCH₂CH₃). ¹³C{¹H} NMR (CD₃CN, 125 MHz, 293 K): δ 257.31 (dd, ²J_{CP} = 27.0, ²J_{CP'} = 1.8 Hz, Mo–CO), 91.46 (s, Cp), 56.21 (dd, ¹J_{CP} = 35.9, ³J_{CP} = 0.7 Hz, PCH₂N), 55.61 (dd, ¹J_{CP} = 39.2, ³J_{CP} = 0.7 Hz, PCH₂N), 50.90 (t, ³J_{CP} = 11.7 Hz, NCH₃), 21.13 (dd, ¹J_{CP} = 22.4, ³J_{CP} = 3.7 Hz, PCH₂CH₃), 20.45 (dd, ¹J_{CP} = 32.5, ³J_{CP} = 2.1 Hz, PCH₂CH₃), 18.83 (dd, ¹J_{CP} = 27.8, ³J_{CP} = 4.9 Hz, PCH₂CH₃), 18.62 (d, ¹J_{CP} = 20.1 Hz, PCH₂CH₃), 7.85 (s, PCH₂CH₃), 7.36 (d, ²J_{CP} = 5.5 Hz, PCH₂CH₃), 6.64 (d, ²J_{CP} =

1.9 Hz, PCH₂CH₃), 6.39 (d, ²J_{CP} = 7.6 Hz, PCH₂CH₃). ³¹P{¹H} NMR (CD₃CN, 202 MHz, 293 K): δ 32.48 (d, ²J_{PP} = 77.7 Hz), 18.51 ppm (d, ²J_{PP} = 77.6 Hz). IR (CH₃CN): $\tilde{\nu}_{\text{CO}}$ 1855 cm⁻¹.

Synthesis of [CpMo(CO)(κ³-P^{Ph}N^{Me}P^{Ph})]⁺[BAR^F₄]⁻. A solution of CpMo(CO)(κ²-P^{Ph}N^{Me}P^{Ph})H (12.3 mg, 20 μmol) in fluorobenzene (0.5 mL) was added to a solution of [Ph₃C]⁺[BAR^F₄]⁻ (22.1 mg, 20 μmol) in fluorobenzene (0.5 mL) at room temperature, resulting in a color change from yellow to red. The solution was layered with pentane (2 mL). Slow diffusion of pentane into the fluorobenzene solution overnight at room temperature gave the product as well-shaped red blocks (many of them suitable for X-ray diffraction). Yield: 21.5 mg (14.6 μmol, 73%).

¹H NMR (C₆D₅Br, 500 MHz, 293 K): δ 8.38 (s, 8H, BAR^F₄), 7.75 (s, 4H, BAR^F₄), 7.52–7.35 (m, 14H, C₆H₅), 7.25 (m, 4H, C₆H₅), 7.11–7.00 (m, 2H, C₆H₅), 5.31 (dd, ³J_{HP} = 14.3, ²J_{HH} = 4.4 Hz, 2H, PCH₂N), 5.04 (s, 5H, Cp), 4.93 (d, ²J_{HP} = 14.1 Hz, 2H, PCH₂N), 2.62 ppm (s, 3H, NCH₃). ¹³C{¹H} NMR (C₆D₅Br, 125 MHz, 293 K): δ 243.97 (t, ²J_{CP} = 22.5 Hz, CO), 162.37 (q, ¹J_{BC} = 49.7 Hz, BAR^F₄ ipso), 133.25 (q, ²J_{CF} = 27.2 Hz, BAR^F₄ ortho), 132.28 (t, ²J_{CP} = 5.4 Hz, C₆H₅), 131.81 (s, C₆H₅), 130.62 (t, ²J_{CP} = 5.4 Hz, C₆H₅), 129.94 (s, C₆H₅), 129.37 (t, ³J_{CP} = 4.8 Hz, C₆H₅), 129.28 (s, C₆H₅), 124.89 (q, ¹J_{CF} = 272.8 Hz, CF₃), 124.19 (d, ³J_{CP} = 3.1 Hz, C₆H₅), 117.84 (quint, ³J_{CF} = 3.6 Hz, BAR^F₄ para), 115.39 (d, ¹J_{CP} = 20.8 Hz, C₆H₅), 92.64 (s, Cp), 79.90 (d, ¹J_{CP} = 14.5 Hz, PCH₂N), 79.58 (d, ¹J_{CP} = 14.7 Hz, PCH₂N), 58.93 (s, NCH₃). BAR^F₄ meta C most likely obscured by C₆D₅Br resonance. ³¹P{¹H} NMR (C₆D₅Br, 202 MHz, 293 K): δ -6.3 ppm (s). IR (fluorobenzene): $\tilde{\nu}_{\text{CO}}$ 1859 cm⁻¹. Anal. Calcd for C₇₇H₅₄BF₂₆MoNOP₂ (including two cocrystallized fluorobenzene solvent molecules, in good accordance with X-ray crystal structure): C, 55.32; H, 3.26; N, 0.84. Found: C, 55.60; H, 3.38; N, 0.95.

Synthesis of [CpMo(CO)(κ²-P^{Et}N^{Me}P^{Et})(H)₂]⁺[B(C₆F₅)₄]⁻. A solution of CpMo(CO)(κ²-P^{Et}N^{Me}P^{Et})H (8.5 mg, 20 μmol) in fluorobenzene (0.5 mL) was precooled to -20 °C in a freezer. [H(OEt)₂]⁺[B(C₆F₅)₄]⁻ (16.6 mg, 20 μmol) was added to the cold solution of CpMo(CO)(κ²-P^{Et}N^{Me}P^{Et})H in fluorobenzene, resulting in a color change from light yellow to almost colorless. The solution was layered with pentane (1 mL). Slow diffusion of pentane into the fluorobenzene solution overnight at -35 °C gave the product as well-shaped off-white needles (many of them suitable for X-ray diffraction). Yield: 18.5 mg (16.8 μmol, 84%). ¹H NMR (fluorobenzene +10% C₆D₆, 500 MHz, 233 K): δ 4.45 (s, 5H, Cp), 2.34–2.19 (m, 2H, PCH₂N), 1.92 (s, 3H, NCH₃), 1.86 (d, ²J_{HP} = 13.8 Hz, 2H, PCH₂N), 1.41–1.29 (m, 2H, CH₂CH₃), 1.23–1.16 (m, 2H, CH₂CH₃), 1.12 (q, ³J_{HH} = 7.8 Hz, 2H, CH₂CH₃), 1.07–1.00 (m, 2H, CH₂CH₃), 0.76 (t, ³J_{HH} = 7.2 Hz, 6H, CH₂CH₃), 0.61 (t, ³J_{HH} = 7.5 Hz, 3H, CH₂CH₃), 0.57 (t, ³J_{HH} = 7.5 Hz, 3H, CH₂CH₃), -5.33 ppm (t, ²J_{HP} = 32.5 Hz, 2H, Mo–H). ³¹P{¹H} NMR (fluorobenzene/toluene-d₈ = 1:1, 202 MHz, 293 K): δ 24.9 ppm (s). ³¹P{¹H} NMR (fluorobenzene/toluene-d₈ = 1:1, 202 MHz, 213 K): δ 26.0 (br s), 22.1 ppm (br s). IR (fluorobenzene): $\tilde{\nu}_{\text{CO}}$ 2037 cm⁻¹. Anal. Calcd for C₄₁H₃₄BF₂₀MoNOP₂: C, 44.55; H, 3.10; N, 1.27. Found: C, 44.68; H, 3.08; N, 1.28.

Attempted Synthesis of [CpMo(CO)(κ²-P^{Ph}N^{Me}P^{Ph})(H)₂]⁺[B(C₆F₅)₄]⁻. A solution of CpMo(CO)(κ²-P^{Ph}N^{Me}P^{Ph})H (12.3 mg, 20 μmol) in fluorobenzene (0.5 mL, with ca. 10% of C₆D₆) was added to a J. Young valve NMR tube and precooled to -35 °C in the freezer. [H(OEt)₂]⁺[B(C₆F₅)₄]⁻ (16.6 mg, 20 μmol) was added to the NMR tube, resulting in a rapid bubbling and gas evolution (presumably H₂). The reaction was monitored by ¹H and ³¹P NMR spectroscopy, which indicated that [CpMo(CO)(κ³-P^{Ph}N^{Me}P^{Ph})]⁺[B(C₆F₅)₄]⁻ was the only product and [CpMo(CO)(κ²-P^{Ph}N^{Me}P^{Ph})(H)₂]⁺[B(C₆F₅)₄]⁻ was too unstable to be observed.

Synthesis of CpMo(CO)(κ²-dppp)H. CpMo(CO)₃H (54.2 mg, 0.22 mmol) was dissolved in hexane (10 mL), and dppp (82.4 mg, 0.20 mmol) was added into the solution. The suspension was heated and stirred at 80 °C for 16 h to give an orange solution. Upon being cooled down to room temperature a large amount of yellow crystals formed. The yellow crystalline solids were washed with hexane (2 × 2 mL) and dried under vacuum. Several of the microneedles were found suitable for X-ray diffraction. Combined yield for *cis* + *trans* isomers:

67.1 mg (0.112 mmol, 56%, *cis:trans* = 1:3). ¹H NMR (CD₂Cl₂, 500 MHz, 293 K): δ 7.64–7.53 (m, 6H, C₆H₅, *cis* + *trans*), 7.50 (t, ³J_{HH} = 6.4 Hz, 1H, C₆H₅, *cis* + *trans*), 7.39 (q, ³J_{HH} = 6.4 Hz, 4H, C₆H₅, *cis* + *trans*), 7.36–7.23 (m, 8H, C₆H₅, *cis* + *trans*), 7.21–7.12 (m, 1H, C₆H₅, *cis* + *trans*), 5.27 (s, 5H, Cp, *trans*), 4.36 (s, 5H, Cp, *cis*), 2.74 (td, ²J_{HP} = 13.8, ³J_{HH} = 7.2 Hz, 2H, PCH₂, *cis* + *trans*), 2.36 (t, ²J_{HP} = 12.5 Hz, 1H, PCH₂, *cis*), 2.20 (t, ²J_{HP} = 11.5 Hz, 2H, PCH₂, *trans*), 2.14–2.05 (m, 2H, PCH₂, *cis*), 1.79–1.59 (m, 1H, PCH₂, *trans*), 1.37–1.23 (m, 1H, PCH₂, *trans*), -5.97 (t, ²J_{HP} = 40.4 Hz, 1H, Mo–H, *cis*), -6.92 (t, ²J_{HP} = 73.4 Hz, 2H, Mo–H, *trans*). ¹³C{¹H} NMR (CD₂Cl₂, 125 MHz, 293 K): δ 251.06 (t, ²J_{CP} = 28.4 Hz, CO, *trans*), 249.53 (dd, ²J_{CP} = 16.5, ²J_{CP'} = 6.7 Hz, CO, *cis*), 144.84 (dd, ¹J_{CP} = 40.1, ³J_{CP} = 2.0 Hz, C₆H₅, *trans*), 142.68 (dd, ¹J_{CP} = 30.7, ³J_{CP} = 5.7 Hz, C₆H₅, *trans*), 138.94 (d, ¹J_{CP} = 39.9 Hz, C₆H₅, *cis*), 137.33 (d, ¹J_{CP} = 43.6 Hz, C₆H₅, *cis*), 133.85 (d, ²J_{CP} = 11.3 Hz, C₆H₅, *cis*), 132.36 (d, ²J_{CP} = 10.8 Hz, C₆H₅, *cis*), 131.74 (t, ²J_{CP} = 4.9 Hz, C₆H₅, *trans*), 131.49 (t, ²J_{CP} = 4.9 Hz, C₆H₅, *trans*), 130.85 (d, ²J_{CP} = 9.4 Hz, C₆H₅, *cis*), 129.51 (d, ²J_{CP} = 8.6 Hz, C₆H₅, *cis*), 129.35 (s, C₆H₅, *cis*), 128.99 (s, C₆H₅, *cis*), 128.77 (s, C₆H₅, *trans*), 128.68 (s, C₆H₅, *trans*), 128.53 (s, C₆H₅, *cis*), 128.20 (s, C₆H₅, *cis*), 127.99 (t, ²J_{CP} = 4.9 Hz, C₆H₅, *trans*), 127.84 (t, ²J_{CP} = 5.9 Hz, C₆H₅, *trans*), 127.12 (d, ²J_{CP} = 9.6 Hz, C₆H₅, *cis*), 89.27 (s, Cp, *trans*), 87.40 (s, Cp, *cis*), 33.63 (d, ¹J_{CP} = 24.0 Hz, PCH₂, *cis*), 32.45 (dd, ¹J_{CP} = 26.4, ³J_{CP} = 8.4 Hz, PCH₂, *trans*), 28.70 (dd, ¹J_{CP} = 17.6, ³J_{CP} = 5.6 Hz, PCH₂, *cis*), 20.98 (s, CH₂CH₂CH₂, *trans*), 18.40 ppm (t, ²J_{CP} = 3.2 Hz, CH₂CH₂CH₂, *cis*). ³¹P{¹H} NMR (CD₂Cl₂, 202 MHz, 293 K): δ 72.46 (s, *trans*), 51.19 ppm (br s, *cis*). ³¹P{¹H} NMR (CD₂Cl₂, 202 MHz, 233 K): δ 72.0 (s, *trans*), 53.5 (d, ²J_{PP} = 64.3 Hz, *cis*), 49.0 ppm (d, ²J_{PP} = 64.5 Hz, *cis*). IR (fluorobenzene): $\tilde{\nu}_{\text{CO}}$ 1813 cm⁻¹. Anal. Calcd for C₃₃H₃₂MoOP₂: C, 65.78; H, 5.35. Found: C, 65.40; H, 5.46.

Synthesis of [CpMo(CO)(κ²-dppp)(H)₂]⁺[B(C₆F₅)₄]⁻. [H(OEt)₂]⁺[B(C₆F₅)₄]⁻ (16.6 mg, 20 μmol) was added to a solution of CpMo(CO)(κ²-dppp)H (12.0 mg, 20 μmol) in fluorobenzene or dichloromethane (0.5 mL), resulting in a color change from light yellow to almost colorless. The solution was layered with pentane (1 mL). Slow diffusion of pentane into the dichloromethane solution overnight at -35 °C gave the product as light orange needles. Yield: 15.6 mg (12.2 μmol, 61%). ¹H NMR (CD₂Cl₂, 500 MHz, 293 K): δ 7.68 (br s, 4H, C₆H₅), 7.55–7.31 (m, 16H, C₆H₅), 4.64 (s, 5H, Cp), 3.12–2.92 (m, 2H, CH₂), 2.60–2.44 (m, 2H, CH₂), 2.35 (t, ³J_{HP} = 14.0 Hz, 2H, CH₂), -3.13 (t, ²J_{HP} = 32.1 Hz, 2H, Mo–H). ³¹P{¹H} NMR (CD₂Cl₂, 202 MHz, 293 K): δ 28.2 ppm (s). ³¹P{¹H} NMR (CD₂Cl₂, 202 MHz, 203 K): δ 30.18 (d, ²J_{PP} = 33.0 Hz), 27.35 ppm (d, ²J_{PP} = 32.8 Hz). IR (fluorobenzene): $\tilde{\nu}_{\text{CO}}$ 1982 cm⁻¹.

■ ASSOCIATED CONTENT

Supporting Information

¹H, ³¹P, and ¹³C NMR spectra; electrochemical data (figures); and crystallographic data (CIF format). The Supporting Information is available free of charge on the ACS Publications website at DOI: 10.1021/acs.inorgchem.5b00728.

■ AUTHOR INFORMATION

Corresponding Author

*E-mail: Morris.Bullock@pnnl.gov.

Notes

The authors declare no competing financial interest.

■ ACKNOWLEDGMENTS

We thank the U.S. Department of Energy, Office of Science, Office of Basic Energy Sciences, Division of Chemical Sciences, Geosciences and Biosciences for support. Pacific Northwest National Laboratory is operated by Battelle for the U.S. Department of Energy. We thank Monte Helm, Elliott Hulley, and Deanna Miller for help on the crystallography; Aaron

Appel for helpful discussions; and Ming Fang for assistance on the electrochemical experiments.

REFERENCES

- (1) (a) Bullock, R. M. *Chem.—Eur. J.* **2004**, *10*, 2366–2374. (b) Bullock, R. M. Ionic Hydrogenations. In *Handbook of Homogeneous Hydrogenation*; de Vries, J. G., Elsevier, C. J., Eds.; Wiley-VCH: Weinheim, Germany, 2007; Chapter 7; Vol. 1, pp 153–197. (c) Rakowski DuBois, M.; DuBois, D. L. *Acc. Chem. Res.* **2009**, *42*, 1974–1982. (d) DuBois, D. L.; Bullock, R. M. *Eur. J. Inorg. Chem.* **2011**, 1017–1027. (e) DuBois, D. L. *Inorg. Chem.* **2014**, *53*, 3935–3960. (f) Bullock, R. M.; Appel, A. M.; Helm, M. L. *Chem. Commun.* **2014**, *50*, 3125–3143.
- (2) (a) Gaus, P. L.; Kao, S. C.; Youngdahl, K.; Darensbourg, M. Y. *J. Am. Chem. Soc.* **1985**, *107*, 2428–2434. (b) Tooley, P. A.; Ovalles, C.; Kao, S. C.; Darensbourg, D. J.; Darensbourg, M. Y. *J. Am. Chem. Soc.* **1986**, *108*, 5465–5470. (c) Kristjánsdóttir, S. S.; Norton, J. R. Acidity of Hydrido Transition Metal Complexes in Solution. In *Transition Metal Hydrides*; Dedieu, A., Ed.; VCH: New York, 1991; Chapter 9, pp 309–359. (d) Eisenberg, D. C.; Norton, J. R. *Isr. J. Chem.* **1991**, *31*, 55–66. (e) Eisenberg, D. C.; Lawrie, C. J. C.; Moody, A. E.; Norton, J. R. *J. Am. Chem. Soc.* **1991**, *113*, 4888–4895. (f) Labinger, J. A. Nucleophilic Reactions of Metal Hydrides. In *Transition Metal Hydrides*; Dedieu, A., Ed.; VCH: New York, 1991; Chapter 10, pp 361–379. (g) Magee, M. P.; Norton, J. R. *J. Am. Chem. Soc.* **2001**, *123*, 1778–1779. (h) Ellis, W. W.; Raebiger, J. W.; Curtis, C. J.; Bruno, J. W.; DuBois, D. L. *J. Am. Chem. Soc.* **2004**, *126*, 2738–2743. (i) Casey, C. P.; Guan, H. *J. Am. Chem. Soc.* **2007**, *129*, 5816–5817. (j) Zhang, G.; Vasudevan, K. V.; Scott, B. L.; Hanson, S. K. *J. Am. Chem. Soc.* **2013**, *135*, 8668–8681.
- (3) (a) Song, J.-S.; Szalda, D. J.; Bullock, R. M.; Lawrie, C. J. C.; Rodkin, M. A.; Norton, J. R. *Angew. Chem., Int. Ed. Engl.* **1992**, *31*, 1233–1235. (b) Bullock, R. M.; Voges, M. H. *J. Am. Chem. Soc.* **2000**, *122*, 12594–12595. (c) Song, J.-S.; Szalda, D. J.; Bullock, R. M. *Organometallics* **2001**, *20*, 3337–3346. (d) Voges, M. H.; Bullock, R. M. *J. Chem. Soc., Dalton Trans.* **2002**, 759–770. (e) Dioumaev, V. K.; Bullock, R. M. *Nature* **2003**, *424*, 530–532. (f) Dioumaev, V. K.; Szalda, D. J.; Hanson, J.; Franz, J. A.; Bullock, R. M. *Chem. Commun.* **2003**, 1670–1671. (g) Kimmich, B. F. M.; Fagan, P. J.; Hauptman, E.; Bullock, R. M. *Chem. Commun.* **2004**, 1014–1015. (h) Kimmich, B. F. M.; Fagan, P. J.; Hauptman, E.; Marshall, W. J.; Bullock, R. M. *Organometallics* **2005**, *24*, 6220–6229. (i) Wu, F.; Dioumaev, V. K.; Szalda, D. J.; Hanson, J.; Bullock, R. M. *Organometallics* **2007**, *26*, 5079–5090.
- (4) (a) Cheng, T.-Y.; Brunschwig, B. S.; Bullock, R. M. *J. Am. Chem. Soc.* **1998**, *120*, 13121–13137. (b) Cheng, T.-Y.; Bullock, R. M. *J. Am. Chem. Soc.* **1999**, *121*, 3150–3155. (c) Cheng, T.-Y.; Bullock, R. M. *Organometallics* **2002**, *21*, 2325–2331.
- (5) Cheng, T.-Y.; Szalda, D. J.; Zhang, J.; Bullock, R. M. *Inorg. Chem.* **2006**, *45*, 4712–4720.
- (6) (a) Xu, W.; Lough, A. J.; Morris, R. H. *Inorg. Chem.* **1996**, *35*, 1549–1555. (b) Ayllon, J. A.; Sayers, S. F.; Sabo-Etienne, S.; Donnadiou, B.; Chaudret, B.; Clot, E. *Organometallics* **1999**, *18*, 3981–3990. (c) Li, H.; Rauchfuss, T. B. *J. Am. Chem. Soc.* **2002**, *124*, 726–727. (d) Curtis, C. J.; Miedaner, A.; Ciancanelli, R.; Ellis, W. W.; Noll, B. C.; Rakowski DuBois, M.; DuBois, D. L. *Inorg. Chem.* **2003**, *42*, 216–227. (e) Ott, S.; Kritikos, M.; Åkermark, B.; Sun, L.; Lomoth, R. *Angew. Chem., Int. Ed.* **2004**, *43*, 1006–1009. (f) Henry, R. M.; Shoemaker, R. K.; DuBois, D. L.; Rakowski DuBois, M. *J. Am. Chem. Soc.* **2006**, *128*, 3002–3010. (g) Ezzaher, S.; Capon, J.-F.; Gloaguen, F.; Pétillon, F. Y.; Schollhammer, P.; Talarmin, J.; Kervarec, N. *Inorg. Chem.* **2009**, *48*, 2–4. (h) Wang, N.; Wang, M.; Liu, J.; Jin, K.; Chen, L.; Sun, L. *Inorg. Chem.* **2009**, *48*, 11551–11558. (i) Olsen, M. T.; Rauchfuss, T. B.; Wilson, S. R. *J. Am. Chem. Soc.* **2010**, *132*, 17733–17740. (j) Liu, T.; Chen, S.; O'Hagan, M. J.; Rakowski DuBois, M.; Bullock, R. M.; DuBois, D. L. *J. Am. Chem. Soc.* **2012**, *134*, 6257–6272. (k) Hulley, E. B.; Welch, K. D.; Appel, A. M.; DuBois, D. L.; Bullock, R. M. *J. Am. Chem. Soc.* **2013**, *135*, 11736–11739. (l) Zheng, D.; Wang, N.; Wang, M.; Ding, S.; Ma, C.; Darensbourg, M. Y.; Hall, M. B.; Sun, L. *J. Am. Chem. Soc.* **2014**, *136*, 16817–16823.
- (7) (a) Lough, A. J.; Park, S.; Ramachandran, R.; Morris, R. H. *J. Am. Chem. Soc.* **1994**, *116*, 8356–8357. (b) Chu, H. S.; Lau, C. P.; Wong, K. Y.; Wong, W. T. *Organometallics* **1998**, *17*, 2768–2777. (c) Lee, D.-H.; Patel, B. P.; Clot, E.; Eisenstein, O.; Crabtree, R. H. *J. Chem. Soc., Chem. Commun.* **1999**, 297–298. (d) Custelcean, R.; Jackson, J. E. *Chem. Rev.* **2001**, *101*, 1963–1980. (e) Olsen, M. T.; Barton, B. E.; Rauchfuss, T. B. *Inorg. Chem.* **2009**, *48*, 7507–7509. (f) Camara, J. M.; Rauchfuss, T. B. *J. Am. Chem. Soc.* **2011**, *133*, 8098–8101. (g) Camara, J. M.; Rauchfuss, T. B. *Nat. Chem.* **2012**, *4*, 26–30. (h) Wang, N.; Wang, M.; Wang, Y.; Zheng, D.; Han, H.; Ahlquist, M. S. G.; Sun, L. *J. Am. Chem. Soc.* **2013**, *135*, 13688–13691. (i) Liu, T.; Wang, X.; Hoffmann, C.; DuBois, D. L.; Bullock, R. M. *Angew. Chem., Int. Ed.* **2014**, *53*, 5300–5304.
- (8) Stephan, G. C.; Näther, C.; Sivasankar, C.; Tuczek, F. *Inorg. Chim. Acta* **2008**, *361*, 1008–1019.
- (9) (a) Bainbridge, A.; Craig, P. J.; Green, M. *J. Chem. Soc. A* **1968**, 2715–2718. (b) Kalck, P.; Pince, R.; Poilblanc, R.; Roussel, J. *J. Organomet. Chem.* **1970**, *24*, 445–452.
- (10) Faller, J. W.; Anderson, A. S. *J. Am. Chem. Soc.* **1970**, *92*, 5852–5860.
- (11) Moore, E. J.; Sullivan, J. M.; Norton, J. R. *J. Am. Chem. Soc.* **1986**, *108*, 2257–2263.
- (12) Fettingner, J. C.; Keogh, D. W.; Pleune, B.; Poli, R. *Inorg. Chim. Acta* **1997**, *261*, 1–5.
- (13) Pleune, B.; Poli, R.; Fettingner, J. C. *Organometallics* **1997**, *16*, 1581–1594.
- (14) Bush, M. A.; Hardy, A. D. U.; Manojlovic-Muir, L.; Sim, G. A. *J. Chem. Soc. A* **1971**, 1003–1009.
- (15) Miyazaki, T.; Tanabe, Y.; Yuki, M.; Miyake, Y.; Nakajima, K.; Nishibayashi, Y. *Chem.—Eur. J.* **2013**, *19*, 11874–11877.
- (16) Bau, R.; Teller, R. G.; Kirtley, S. W.; Koetzle, T. F. *Acc. Chem. Res.* **1979**, *12*, 176–183.
- (17) Ryan, O. B.; Tilset, M.; Parker, V. D. *J. Am. Chem. Soc.* **1990**, *112*, 2618–2626.
- (18) Smith, K.-T.; Tilset, M. *J. Organomet. Chem.* **1992**, *431*, 55–64.
- (19) Quadrelli, E. A.; Kraatz, H.-B.; Poli, R. *Inorg. Chem.* **1996**, *35*, 5154–5162.
- (20) Fettingner, J. C.; Kraatz, H.-B.; Poli, R.; Quadrelli, E. A.; Torralba, R. C. *Organometallics* **1998**, *17*, 5767–5775.
- (21) Cheng, T.-Y.; Szalda, D. J.; Hanson, J. C.; Muckerman, J. T.; Bullock, R. M. *Organometallics* **2008**, *27*, 3785–3795.
- (22) van der Eide, E. F.; Yang, P.; Bullock, R. M. *Angew. Chem., Int. Ed.* **2013**, *52*, 10190–10194.
- (23) Mock, M. T.; Chen, S.; Rousseau, R.; O'Hagan, M. J.; Dougherty, W. G.; Kassel, W. S.; DuBois, D. L.; Bullock, R. M. *Chem. Commun.* **2011**, 47, 12212–12214.
- (24) Hulley, E. B.; Helm, M. L.; Bullock, R. M. *Chem. Sci.* **2014**, *5*, 4729–4741.
- (25) (a) Kane, J. C.; Wong, E. H.; Yap, G. P. A.; Rheingold, A. L. *Polyhedron* **1999**, *18*, 1183–1188. (b) Sanchez Ballester, N. M.; Elsegood, M. R. J.; Smith, M. B.; Brown, G. M. *Acta Crystallogr., Sect. E* **2007**, *63*, m719–m721. (c) Stephan, G.; Nather, C.; Tuczek, F. *Acta Crystallogr., Sect. E* **2008**, *64*, m629. (d) Latypov, S. K.; Strelnik, A. G.; Ignatieva, S. N.; Hey-Hawkins, E.; Balueva, A. S.; Karasik, A. A.; Sinyashin, O. G. *J. Phys. Chem. A* **2012**, *116*, 3182–3193. (e) Weiss, C. J.; Groves, A. N.; Mock, M. T.; Dougherty, W. G.; Kassel, W. S.; Helm, M. L.; DuBois, D. L.; Bullock, R. M. *Dalton Trans.* **2012**, *41*, 4517–4529.
- (26) Garrou, P. E. *Chem. Rev.* **1981**, *81*, 229–266.
- (27) (a) Brookhart, M.; Cox, K.; Cloke, F. G. N.; Green, J. C.; Green, M. L. H.; Hare, P. M.; Bashkin, J.; Derome, A. E.; Grebenik, P. D. *J. Chem. Soc., Dalton Trans.* **1985**, 423–433. (b) Dai, Q. X.; Seino, H.; Mizobe, Y. *Eur. J. Inorg. Chem.* **2011**, *2011*, 141–149. (c) Buss, J. A.; Edouard, G. A.; Cheng, C.; Shi, J.; Agapie, T. *J. Am. Chem. Soc.* **2014**, *136*, 11272–11275. (d) Yasuda, R.; Iwasa, K.; Niikura, F.; Seino, H.; Mizobe, Y. *Dalton Trans.* **2014**, *43*, 9344–9355.

- (28) (a) Desrosiers, P. J.; Cai, L.; Lin, Z.; Richards, R.; Halpern, J. J. *Am. Chem. Soc.* **1991**, *113*, 4173–4184. (b) Janak, K. E.; Shin, J. H.; Parkin, G. J. *Am. Chem. Soc.* **2004**, *126*, 13054–13070. (c) Pons, V.; Conway, S. L. J.; Green, M. L. H.; Green, J. C.; Herbert, B. J.; Heinekey, D. M. *Inorg. Chem.* **2004**, *43*, 3475–3483. (d) Baya, M.; Houghton, J.; Daran, J.-C.; Poli, R.; Male, L.; Albinati, A.; Gutman, M. *Chem.—Eur. J.* **2007**, *13*, 5347–5359. (e) Dub, P. A.; Baya, M.; Houghton, J.; Belkova, N. V.; Daran, J.-C.; Poli, R.; Epstein, L. M.; Shubina, E. S. *Eur. J. Inorg. Chem.* **2007**, *2007*, 2813–2826. (f) Kubas, G. J. *Chem. Rev.* **2007**, *107*, 4152–4205. (g) Baya, M.; Dub, P. A.; Houghton, J.; Daran, J.-C.; Belkova, N. V.; Shubina, E. S.; Epstein, L. M.; Lledós, A.; Poli, R. *Inorg. Chem.* **2008**, *48*, 209–220. (h) Dub, P. A.; Belkova, N. V.; Filippov, O. A.; Daran, J.-C.; Epstein, L. M.; Lledós, A.; Shubina, E. S.; Poli, R. *Chem.—Eur. J.* **2010**, *16*, 189–201.
- (29) (a) Jessop, P. G.; Morris, R. H. *Coord. Chem. Rev.* **1992**, *121*, 155–284. (b) Heinekey, D. M.; Oldham, W. J., Jr. *Chem. Rev.* **1993**, *93*, 913–926. (c) Johnson, C. E.; Fisher, B. J.; Eisenberg, R. J. *Am. Chem. Soc.* **1983**, *105*, 7772–7774. (d) Fryzuk, M. D.; MacNeil, P. A. *Organometallics* **1983**, *2*, 682–684. (e) Lee, J. C., Jr.; Peris, E.; Rheingold, A. L.; Crabtree, R. H. *J. Am. Chem. Soc.* **1994**, *116*, 11014–11019. (f) Peris, E.; Lee, J. C., Jr.; Rambo, J. R.; Eisenstein, O.; Crabtree, R. H. *J. Am. Chem. Soc.* **1995**, *117*, 3485–3491. (g) Kubas, G. J. *Metal Dihydrogen and σ -Bond Complexes: Structure, Theory, and Reactivity*; Kluwer Academic/Plenum Publishers: New York, 2001.
- (30) Bullock, R. M.; Song, J.-S.; Szalda, D. J. *Organometallics* **1996**, *15*, 2504–2516.
- (31) (a) Tilset, M. *J. Am. Chem. Soc.* **1992**, *114*, 2740–2741. (b) Ciancanelli, R.; Noll, B. C.; DuBois, D. L.; DuBois, M. R. *J. Am. Chem. Soc.* **2002**, *124*, 2984–2992. (c) Miedaner, A.; Raebiger, J. W.; Curtis, C. J.; Miller, S. M.; DuBois, D. L. *Organometallics* **2004**, *23*, 2670–2679. (d) Raebiger, J. W.; DuBois, D. L. *Organometallics* **2005**, *24*, 110–118. (e) Roberts, J. A. S.; Appel, A. M.; DuBois, D. L.; Bullock, R. M. *J. Am. Chem. Soc.* **2011**, *133*, 14604–14613.
- (32) Connelly, S. J.; Kaminsky, W.; Heinekey, D. M. *Organometallics* **2013**, *32*, 7478–7481.
- (33) Jutzi, P.; Müller, C.; Stämmler, A.; Stämmler, H.-G. *Organometallics* **2000**, *19*, 1442–1444.
- (34) (a) Tate, D. P.; Knipple, W. R.; Augl, J. M. *Inorg. Chem.* **1962**, *1*, 433–434. (b) Behrens, U.; Edelmann, F. *J. Organomet. Chem.* **1984**, *263*, 179–182.
- (35) Keppie, S. A.; Lappert, M. F. *J. Chem. Soc. A* **1971**, 3216–3220.
- (36) SAINT, v. 7.68A; Bruker AXS Inc.: Madison, WI, 2010.
- (37) Sheldrick, G. M. SADABS, v. 2008/1; Bruker AXS Inc.: Madison, WI, 2010.
- (38) Sheldrick, G. M. *Acta Crystallogr., Sect. A: Found. Adv.* **2008**, *64*, 112–122.
- (39) Farrugia, L. J. *J. Appl. Crystallogr.* **1997**, *30*, 565.
- (40) Dolomanov, O. V.; Bourhis, L. J.; Gildea, R. J.; Howard, J. A. K.; Puschmann, H. *J. Appl. Crystallogr.* **2009**, *42*, 339–341.